

# Non-perturbative effects in the energy-energy correlation

---

**Yu.L. Dokshitzer\*, G. Marchesini,**

*Dipartimento di Fisica, Università di Milano-Bicocca  
and INFN, Sezione di Milano, Italy*

**B.R. Webber**

*Cavendish Laboratory, University of Cambridge  
Madingley Road, Cambridge CB3 0HE, UK*

**ABSTRACT:** The fully resummed next-to-leading-order perturbative calculation of the energy-energy correlation in  $e^+e^-$  annihilation is extended to include the leading non-perturbative power-behaved contributions computed using the “dispersive method” applied earlier to event shape variables. The correlation between a leading (anti)quark and a gluon produces a non-perturbative  $1/Q$  contribution, while non-perturbative effects in the quark-antiquark correlation give rise to a smaller contribution  $\ln Q^2/Q^2$ . In the back-to-back region, the power-suppressed contributions actually decrease much more slowly, as small non-integer powers of  $1/Q$ , as a result of the interplay with perturbative effects. The hypothesis of a universal low-energy form for the strong coupling relates the coefficients of these contributions to those measured for other observables.

**KEYWORDS:** QCD, NLO Computations, Jets, LEP and SLC Physics.

---

\*On leave from St. Petersburg Nuclear Institute, Gatchina, St. Petersburg 188350, Russia

---

## Contents

<b>1. Introduction</b>	<b>2</b>
<b>2. Kinematics and resummation</b>	<b>4</b>
2.1 Kinematics in the soft limit	5
2.2 Resummation of soft contributions	6
<b>3. Soft emission radiator</b>	<b>8</b>
3.1 PT part of the radiator	9
3.2 NP part of the radiator	10
<b>4. Quark-gluon correlation</b>	<b>11</b>
4.1 PT contribution	12
4.2 NP contribution	12
<b>5. Final results</b>	<b>15</b>
5.1 Matching resummed and fixed-order predictions	15
5.2 Merging PT and NP contributions	17
<b>6. Comparison with experiment</b>	<b>18</b>
<b>7. Discussion</b>	<b>20</b>
<b>A. Radiator</b>	<b>23</b>
A.1 Phase space and momentum balance	23
A.2 One-loop radiator	25
A.3 Two-loop radiator	26
<b>B. Quark-gluon contributions</b>	<b>29</b>
<b>C. Perturbative analysis of subleading corrections</b>	<b>32</b>
C.1 Single-log corrections to the radiator	32
C.2 Perturbative $q\bar{q}$ contribution	34
<b>D. Analytical estimates using one-loop coupling</b>	<b>35</b>
D.1 Perturbative $q\bar{q}$ distribution	36
D.2 Full $q\bar{q}$ distribution	37
D.3 NP $q\bar{q}$ contribution	38
D.4 Full EEC	39

---

# 1. Introduction

The energy-energy correlation [1] (EEC) in  $e^+e^-$  annihilation was one of the first collinear and infrared safe observables [2] for which the all-order resummation of perturbative (PT) radiative corrections proved to be necessary, in the back-to-back (as well as in the forward) kinematical configuration [3–5]. It was soon noticed that the comparison of the theoretical prediction with the data required the introduction of sizeable non-perturbative (NP) corrections. A simple model for NP effects, already proposed by Basham et al. in 1979 [1], suggested that they should scale as  $1/Q$ ,  $Q$  being the total annihilation energy (hardness scale). A more detailed model for NP corrections to the EEC was suggested by Collins and Soper in 1985 [6]. Operationally, they suggested modelling the NP effects due to the transition from partons to hadrons as a kind of smearing of the PT distribution.

In recent years power-suppressed NP contributions were studied for a wide variety of hard cross sections [7]. In particular,  $1/Q$  contributions were predicted and phenomenologically quantified for a number of jet shape observables such as thrust and jet masses, the  $C$ -parameter and jet broadenings (for a review see [8]). Following the technique for analysing the power-behaved contributions to hard observables developed in [9], we are now in a position to better understand the NP effects in the EEC distribution and to relate the corresponding NP parameters with those emerging from the analyses of jet shapes. This is the main purpose of the present article.

Let us start by recalling that the energy-energy correlation (EEC) is defined as

$$\begin{aligned} \frac{d\Sigma(\chi)}{d\cos\chi} &\equiv \frac{d\sigma}{\sigma d\cos\chi} = \sum_n \int \frac{d\sigma_n}{\sigma} \text{EEC}(\chi), \\ \text{EEC}(\chi) &= \sum_{a,b} \frac{E_a E_b}{Q^2} \delta(\cos\chi + \cos\Theta_{ab}), \end{aligned} \tag{1.1}$$

where the sums are over all final-state particles  $a$  and  $b$ , so that each pair of particles is counted twice. Here  $\chi = \pi - \Theta_{ab}$  so that in the back-to-back region  $\chi \ll 1$ .

Perturbatively, the correlation is dominated by the contribution from the primary  $q\bar{q}$  pair, while the  $qg$  correlation produces a subleading correction.

At the non-perturbative level, there are two physically different confinement effects in the EEC. The first is an additional NP contribution to the  $q\bar{q}$  angular imbalance due to radiation of secondary gluons with transverse momenta of the order of  $\Lambda_{\text{QCD}}$ , which we call *gluers* [10]. This contribution scales as  $1/Q^2$ . A more important NP contribution comes from the correlation between the (anti)quark and a *gluer* with  $E_g \sim \Lambda_{\text{QCD}}/\chi$ , which scales as  $1/(Q\chi)$ . As a result of an interplay between the NP and PT effects in the EEC distribution, the naive dimensions  $1/Q$  and  $1/Q^2$  get modified, in the back-to-back region, and the power-suppressed contributions decrease with  $Q$  much more slowly.

At the parton level, the quark-quark contribution to the integrated distribution  $\Sigma(\chi)$  for small values of  $t = \tan(\frac{1}{2}\chi)$  has the structure (to leading-logarithmic order)

$$\Sigma_{q\bar{q}}(\chi) = f(\alpha_s \log^2 t).$$

The contribution from the (anti)quark–gluon correlation is one log down:

$$\Sigma_{qg}(\chi) \sim \alpha_s \log \frac{1}{t} \cdot f(\alpha_s \log^2 t).$$

The single-logarithmic enhancement here comes from the collinear singularity of the  $qg$  matrix element at  $t = 0$ . However it can be effectively absorbed into the  $q\bar{q}$  contribution. Indeed, adding the energies of the quark and the gluon(s) *collinear* with it produces the initial quark energy, so that these two terms together correspond to neglecting the quark energy loss in the  $q\bar{q}$  correlation. Having performed the collinear subtraction, one is left with the residual  $qg$  contribution to  $\Sigma$  at the level of a correction of relative order  $\alpha_s$ . Analogously, the correlation between two secondary gluons starts at the  $\alpha_s^2$  level and will be neglected hereafter in the derivation of the resummed next-to-leading PT distribution<sup>1</sup>.

As a result, the EEC at small  $\chi$ , at the perturbative level, can be simply treated by considering the correlation between the primary quark and the antiquark, which are no longer aligned, because of multiple gluon bremsstrahlung, but do not lose energy.

At the NP level, the leading power-behaved contribution due to the quark-gluon correlation is proportional to

$$\Sigma_{qg}^{(\text{NP})}(\chi) \propto \langle b \rangle \cdot \Sigma_{q\bar{q}}^{(\text{PT})}(\chi),$$

where  $\langle b \rangle$ , depending on  $Q$  and the angle between the two energy detectors, is the characteristic value of the impact parameter determining the PT distribution. In the back-to-back limit,  $\chi = \pi - \theta \rightarrow 0$ , one observes a power behaviour,  $\langle b \rangle \propto Q^{-\gamma-1}$  with a non-integer anomalous dimension  $\gamma$  [5]. As a result, the leading NP correction to the height of the perturbative EEC plateau at  $\chi = 0$  becomes

$$\frac{d\Sigma^{(\text{NP})}}{d\cos\chi}(\chi=0) \propto \frac{d\Sigma^{(\text{PT})}}{d\cos\chi}(\chi=0) \cdot Q^{-\gamma}.$$

The non-integer exponent depends on the treatment of the PT coupling. In particular, for the one-loop coupling with  $n_f = 3(5)$  we obtain  $\gamma \simeq 0.32(0.36)$  (see Appendix D.3).

The final expression for the EEC which accounts for the leading power effects has the following structure. After extracting a kinematical factor and the “coefficient

---

<sup>1</sup>The  $\mathcal{O}(\alpha_s^2)$  PT corrections coming from the  $gg$  EEC, as well as from other sources, are taken care of by matching the approximate logarithmic distribution with the exact two-loop matrix element calculation, performed in Section 5.1.

function” factor  $C = 1 + \mathcal{O}(\alpha_s)$ , we are left with an expression based on the “radiator”  $\mathcal{R}(b)$ , which exponentiates in impact parameter space,

$$\begin{aligned} \frac{d\Sigma}{d\cos\chi} &= C(\alpha_s) \frac{(1+t^2)^3}{4} \mathcal{I}(t), \\ \mathcal{I}(t) &= \frac{Q^2}{2} \int b db J_0(bQt) e^{-\mathcal{R}(b)} (1 - 2b\lambda + \mathcal{O}(b^2\Lambda_{\text{QCD}}^2)). \end{aligned} \quad (1.2)$$

The linear NP correction  $-2b\lambda$  originates from the quark-gluon correlation, where  $\lambda$  is a parameter (with the dimension of mass) which characterises the NP interaction at small momentum scales,

$$\lambda = \frac{4C_F}{\pi^2} \mathcal{M} \int_0^\infty dk \alpha_s^{(\text{NP})}(k). \quad (1.3)$$

The issue of the PT–NP matching is explained in Sect. 5.2, and the origin of the Milan factor  $\mathcal{M}$  is recalled in Appendix B.

The radiator in (1.2) contains its own NP component which is *quadratic* in  $b$ ,

$$\begin{aligned} \mathcal{R}(b) &= \mathcal{R}^{(\text{PT})}(b) + \frac{1}{2}b^2\sigma, \\ \sigma &= \frac{C_F}{2\pi} \int_0^\infty dk^2 \left( \ln \frac{Q^2}{k^2} - \frac{1}{2} \right) \alpha_s^{(\text{NP})}(k), \end{aligned} \quad (1.4)$$

Strictly speaking, this contribution should have been dropped since we did not analyse a comparable quadratic effect which may come from the  $qg$  correlation. However we choose to keep the  $\sigma$  effect for two reasons. Firstly, it allows us to verify that this quadratic NP term affects the result much less than the leading  $b\lambda$  contribution. Secondly, the  $\sigma$  contribution is logarithmically enhanced in  $Q$ , which enhancement should not necessarily be present in the next-to-leading power contribution from the  $qg$  correlation. A complete analysis of  $1/Q^2$  effects in the EEC remains to be done.

In the present paper we give a comparison of available data with theoretical expectations based on “default” values of the relevant NP parameters, without attempting a fit to extract the optimal values. Our aim is to stimulate more detailed experimental studies of the EEC in the back-to-back region, where there is a particularly interesting interplay between perturbative and non-perturbative dynamics.

## 2. Kinematics and resummation

In this section, after introducing the energy-energy correlation and the kinematics, we recall the relevant results of resummation in the soft limit which are needed for power correction studies. To this end, one needs to consider also the contributions coming from the reconstruction of the running coupling at large distances. They are obtained by using the dispersive method discussed in [9]. The specific calculations for the EEC are similar to the ones performed for shape variables (see [11]). They are described in detail in Appendix A.

## 2.1 Kinematics in the soft limit

At the parton level, the quantity EEC receives contributions from the primary quark  $p$  and antiquark  $\bar{p}$  and the *secondary* partons  $k_i$ . In the soft limit the primary quark and antiquark belong to opposite hemispheres. Neglecting the products of energies  $\omega_i$  of the secondary partons, we have

$$Q^2 \cdot \text{EEC}(\chi) = 2E\bar{E}\delta(\cos\chi + \cos\Theta_{p\bar{p}}) + 4\sum_{i=1}^n E\omega_i\delta(\cos\chi + \cos\Theta_{pi}) + \mathcal{O}(\omega_i\omega_j), \quad (2.1)$$

where we have used the quark-antiquark symmetry of the matrix element.

For the parton momenta we use the Sudakov decomposition. Introducing two light-light opposite vectors  $P$  and  $\bar{P}$ , we write

$$p = \zeta P, \quad \bar{p} = \sigma P + \rho\bar{P} + p_t, \quad k_i = \beta_i P + \alpha_i\bar{P} + k_{ti}, \quad (2.2)$$

where we have taken  $P$  along the quark direction and  $2P\bar{P} = Q^2$ . In the soft limit all quantities

$$\alpha_i, \beta_i, 1 - \zeta, 1 - \rho, \frac{k_{ti}}{Q},$$

are small and of the same order, while  $\sigma$  is much smaller (quadratic in  $p_t/Q$ ). Neglecting quadratic soft terms, we have

$$\begin{aligned} \text{EEC} &\simeq \frac{(1+t^2)^2}{4} \left\{ \zeta(\rho + \sigma)\delta\left(t^2 - \frac{p_t^2}{Q^2\rho^2}\right) + 2\sum_i(\alpha_i + \beta_i)\delta\left(t^2 - \frac{k_{ti}^2}{Q^2\alpha_i^2}\right) \right\} \\ &= \frac{(1+t^2)^3}{4} \left\{ \rho\zeta\delta\left(t^2 - \frac{p_t^2}{Q^2\rho^2}\right) + 2\sum_i\alpha_i\delta\left(t^2 - \frac{k_{ti}^2}{Q^2\alpha_i^2}\right) \right\}. \end{aligned} \quad (2.3)$$

Here we have used  $\alpha_i\beta_i = k_{ti}^2/Q^2$ ,  $\sigma\rho = p_t^2/Q^2$  and

$$t = \tan\frac{\pi - \theta}{2} \equiv \tan\frac{\chi}{2}, \quad \tan\frac{\pi - \theta_{p\bar{p}}}{2} = \frac{p_t}{Q\rho}, \quad \tan\frac{\pi - \theta_{pk_i}}{2} = \frac{k_{ti}}{Q\alpha_i}.$$

The expression (2.3) takes into account the recoil of the quark-antiquark ( $\rho\zeta \neq 1$  and  $p_t \neq 0$ ) against (soft) secondary partons. It can be cast in a more transparent form by using

$$\rho\zeta = \left(1 - \sum_i\alpha_i\right) \left(1 - \sigma - \sum_i\beta_i\right) = 1 - \sum_i\alpha_i - \sum_i\beta_i + \dots \quad (2.4)$$

where the dots correspond to terms quadratic in the soft scale. Finally, using the fact that the matrix element is symmetric with respect to exchange of  $\alpha_i$  and  $\beta_i$ , we

can write (apart from quadratic soft terms)

$$\text{EEC} = \frac{(1+t^2)^3}{4} \left\{ \delta \left( t^2 - \frac{p_t^2}{Q^2 \rho^2} \right) + 2 \sum_i \alpha_i \left[ \delta \left( t^2 - \frac{k_{ti}^2}{Q^2 \alpha_i^2} \right) - \delta \left( t^2 - \frac{p_t^2}{Q^2 \rho^2} \right) \right] \right\}. \quad (2.5)$$

This form explicitly shows that the quantity EEC is infrared and collinear safe. In particular, it remains finite when a secondary gluon happens to be collinear with the antiquark momentum,  $\vec{\kappa}_{ti} \rightarrow 0$ ,

$$\vec{\kappa}_{ti} \equiv \vec{k}_{ti} - \frac{\alpha_i}{\rho} \vec{p}_t, \quad (2.6)$$

where the matrix element has collinear singularities (see Appendix A.2):

$$|M^2| \propto \left( \frac{2(pk_i)(k_i \bar{p})}{(p\bar{p})} \right)^{-1} = \frac{1}{\kappa_{ti}^2} \rightarrow \infty. \quad (2.7)$$

Indeed, the first term on the right-hand side of (2.5) does not depend on the secondary parton (gluon) variables. As a result, collinear and soft divergences of the radiation probability cancel, in the standard way, in the inclusive sum of real and virtual contributions. The second term is proportional to the secondary parton momentum,  $\alpha_i$ , and therefore is present only in the real contribution (quark-gluon correlation). Here the *soft* singularity of the matrix element,  $d\alpha_i/\alpha_i$ , is damped by the  $\alpha_i$  factor, while the *collinear* singularity,  $\vec{\kappa}_{ti} \rightarrow 0$ , is regularised by the vanishing difference of the delta functions in the square brackets, the direct quark-gluon contribution to the correlation and the subtraction term due to the antiquark energy loss which was not included into the first term, see (2.4).

Hereafter we shall refer to the two terms in (2.5) as the  $q\bar{q}$  and  $qg$  contributions to the EEC, respectively. Thus reorganised, the  $q\bar{q}$  contribution dominates the PT answer, while the  $qg$  one gives rise to the leading  $1/Q$  NP correction.

## 2.2 Resummation of soft contributions

Resummation of multiple soft gluon radiation off the  $q\bar{q}$  antenna is necessary (and sufficient, in the leading order) for describing the EEC in the back-to-back (small  $t$ ) region. In this approximation the partial cross sections can be factorized as

$$\frac{d\sigma_n}{\sigma} = C(\alpha_s) dw_n. \quad (2.8)$$

Here  $dw_n$  stands for the normalized  $n$  soft parton emission probability, and the ‘‘coefficient function’’  $C(\alpha_s) = 1 + \mathcal{O}(\alpha_s(Q))$  is included in order to match the soft-resummed expression with the exact two-loop result. According to (2.5), the observable (1.1) acquires two contributions

$$\frac{d\sigma}{\sigma d\cos\chi} = C(\alpha_s) \frac{(1+t^2)^3}{4} \mathcal{I}(t), \quad \mathcal{I}(t) = \mathcal{I}_{q\bar{q}}(t) + \mathcal{I}_{qg}(t), \quad (2.9)$$

where

$$\mathcal{I}_{q\bar{q}}(t) = \sum_n \int dw_n \delta\left(t^2 - \frac{\vec{p}_t^2}{Q^2 \rho^2}\right), \quad (2.10)$$

$$\mathcal{I}_{qg}(t) = 2 \sum_n \int dw_n \sum_i \alpha_i \left[ \delta\left(t^2 - \frac{k_{ti}^2}{Q^2 \alpha_i^2}\right) - \delta\left(t^2 - \frac{p_t^2}{Q^2 \rho^2}\right) \right]. \quad (2.11)$$

The distribution  $\mathcal{I}_{qg}(t)$  includes the recoiling part of the  $q\bar{q}$  contribution (second term in the square bracket) so that, as observed before, the collinear singularities in  $dw_n$  for  $\vec{\kappa}_{ti} \rightarrow 0$  are cancelled.

In Appendix A.2 we discuss in detail the soft parton emission probabilities  $dw_n$ . They depend on the secondary parton momenta  $\vec{\kappa}_{ti}$  defined in (2.6) and on the rescaled antiquark momentum

$$\vec{p} = \frac{\vec{p}_t}{\rho} \quad (2.12)$$

and have the form<sup>2</sup>

$$dw_n = d^2p \int \frac{d^2b}{(2\pi)^2} e^{i\vec{b}\vec{p}} dW_n(\{\vec{\kappa}_{ti}, \alpha_i\}; \vec{b}), \quad (2.13)$$

where the distributions  $dW_n$  are factorized in the momenta of the secondary soft partons. To obtain such a factorization one needs to introduce the integration over the impact parameter  $\vec{b}$  to represent the transverse momentum conservation

$$\delta^2(\vec{p}_t + \sum_i \vec{k}_{ti}) = \delta^2(\vec{p} + \sum_i \vec{\kappa}_{ti}) = \int \frac{d^2b}{(2\pi)^2} e^{i\vec{b}\vec{p}} \prod_i e^{i\vec{b}\vec{\kappa}_{ti}}. \quad (2.14)$$

The factorization of  $dW_n$  allows the soft parton resummation. In particular one has

$$\sum_n \int dW_n(\{\vec{\kappa}_{ti}, \alpha_i\}; \vec{b}) = e^{-\mathcal{R}(b)}, \quad \mathcal{R}(0) = 0, \quad (2.15)$$

with  $\mathcal{R}(b)$  the soft emission radiator.

The distributions  $dW_n$  are singular for  $\kappa_{ti} \rightarrow 0$  and  $\alpha_i \rightarrow 0$ . At inclusive level, these singularities cancel against corresponding singularities in the virtual contributions resummed by Sudakov form factors included into  $dW_n$ . As a result, the radiator is collinear and infrared finite.

From (2.15) we immediately obtain the  $q\bar{q}$  contribution  $\mathcal{I}_{q\bar{q}}(t)$  (see (2.10))

$$\mathcal{I}_{q\bar{q}}(t) = \frac{Q^2}{2} \int b db J_0(Qbt) e^{-\mathcal{R}(b)}. \quad (2.16)$$

---

<sup>2</sup>the  $\{\vec{\kappa}_{ti}, \alpha_i\}$  variables are convenient for describing partons in the *right* hemisphere, i.e. the one opposite to the triggered quark, see below.



Notice the normalization that in the limit of no secondary emission,  $\mathcal{R} \rightarrow 0$ , one has  $\mathcal{I}_{q\bar{q}}(t) \rightarrow \delta(t^2)$ .

The ‘‘quark-gluon’’ EEC,  $\mathcal{I}_{qg}(t)$ , receives contributions from each one of the secondary partons (see (2.11)). Due to the factorization of  $dW_n$  the sum can again be expressed in terms of the resummed distribution based on the standard radiator, with the triggered parton singled out. The details can be found in Appendix B.

### 3. Soft emission radiator

In this section we analyse the radiator, which contains both PT and NP contributions.

The essential point is the reconstruction of the running coupling, which requires a two-loop analysis. To this accuracy the radiator is given by the contributions of one and two soft partons and has the form (see [11])

$$\mathcal{R}(b) = \int d\omega_1(k) [1 - J_0(b\kappa_t)] + \int d\omega_2(k_1 k_2) [1 - J_0(b|\vec{\kappa}_{t1} + \vec{\kappa}_{t2}|)], \quad (3.1)$$

where  $d\omega_1$  is the one ‘‘real’’ soft gluon emission distribution with one-loop virtual correction included;  $d\omega_2$  is the two non-independent ‘‘real’’ soft parton emission distribution. The precise expressions for  $d\omega_1$  and  $d\omega_2$  are recalled in Appendix A.3. Notice that the last contribution is inclusive, i.e. the sum  $\vec{\kappa}_{t1} + \vec{\kappa}_{t2}$  enters as argument of the Bessel function.

The most natural way the running coupling appears in Minkowskian observables [12] is through the dispersive relation,

$$\frac{\alpha_s(k)}{k^2} = \int_0^\infty \frac{dm^2}{(m^2 + k^2)^2} \alpha_{\text{eff}}(m), \quad (3.2)$$

where the effective coupling [9],  $\alpha_{\text{eff}}(m)$ , is the primitive function of the discontinuity of  $\alpha_s(m)$ . In the PT region,  $m^2 \gg \Lambda^2$ , the effective coupling  $\alpha_{\text{eff}}(m)$  differs from the standard  $\alpha_s(m)$  by  $\mathcal{O}(\alpha_s^3)$ . It is important to stress that the relation (3.2) is supposed to be applicable both for large and small momentum scales, and thus makes it possible to quantify the NP contribution to the radiator.

By using the representation (3.2) we reconstruct the running coupling in the radiator and obtain the following expression, see Appendix A.3,

$$\mathcal{R}(b) = \frac{C_F}{\pi} \int_0^{Q^2} dm^2 \alpha_{\text{eff}}(m) \frac{-d}{dm^2} \int_0^{Q^2} \frac{d\kappa_t^2}{m^2 + \kappa_t^2} [1 - J_0(b\kappa_t)] \ln \frac{Q^2 e^{-\frac{3}{2}}}{m^2 + \kappa_t^2}. \quad (3.3)$$

First we recall the PT result and then derive the leading NP part of  $\mathcal{R}(b)$ .

### 3.1 PT part of the radiator

By using (3.2) we show in Appendix A.3 that the PT part of (3.3) reproduces the well known next-to-leading expression [13]

$$\mathcal{R}^{(\text{PT})}(b) = \frac{C_F}{\pi} \int_0^{Q^2} \frac{d\kappa_t^2}{\kappa_t^2} \alpha_s^{\text{PT}}(\kappa_t) [1 - J_0(b\kappa_t)] \ln \frac{Q^2 e^{-\frac{3}{2}}}{\kappa_t^2}. \quad (3.4)$$

Here the two-loop PT coupling  $\alpha_s^{\text{PT}}(\kappa_t)$  is taken in the physical ‘‘bremsstrahlung’’ scheme, in which the coupling is defined as the intensity of soft gluon radiation [14]. Since the observable is collinear and infrared finite, the  $1/\kappa_t^2$  singularity is regularized by the factor  $[1 - J_0(b\kappa_t)]$ . In (3.4) we must keep  $\kappa_t^2 > \Lambda_{\text{QCD}}^2$ .

The explicit expression for the PT radiator with the next-to-leading accuracy was derived in [15]. It is obtained by replacing the factor  $[1 - J_0(b\kappa_t)]$  by the theta-function, see Appendix C.1,

$$\mathcal{R}^{(\text{PT})}(b) \simeq \frac{C_F}{\pi} \int_0^{Q^2} \frac{d\kappa_t^2}{\kappa_t^2} \alpha_s^{\text{PT}}(\kappa_t) \ln \frac{Q^2 e^{-\frac{3}{2}}}{\kappa_t^2} \cdot \vartheta \left( \kappa_t - \frac{2}{be^{\gamma_E}} \right). \quad (3.5)$$

This gives

$$\begin{aligned} \mathcal{R}^{(\text{PT})}(b) = & -\frac{16\pi C_F}{\beta_0^2} \left[ \frac{1}{\alpha_s} (\ln(1-\ell) + \ell) - \frac{3\beta_0}{8\pi} \ln(1-\ell) \right. \\ & \left. + \frac{\beta_1}{4\pi\beta_0} \left( \frac{1}{2} \ln^2(1-\ell) + \frac{\ln(1-\ell)}{1-\ell} + \frac{\ell}{1-\ell} \right) \right], \end{aligned} \quad (3.6)$$

where

$$\ell = \beta_0 \frac{\alpha_s}{2\pi} \ln \frac{bQe^{\gamma_E}}{2}, \quad \beta_0 = \frac{11N_c}{3} - \frac{2n_f}{3}, \quad \beta_1 = 102 - \frac{38n_f}{3}, \quad (3.7)$$

and  $\alpha_s$  means  $\alpha_s(Q)$  in the bremsstrahlung scheme [14]. The first line corresponds to the contribution from the one-loop running coupling. The radiators with the two-loop and one-loop  $\alpha_s$  differ at the level of an  $\mathcal{O}(\alpha_s^3 \ln^3 b)$  term which is under control and should be kept in the PT distributions.

The expression (3.6) only makes sense for  $0 < \ell < 1$ , that is, for  $b_{\min} < b < b_{\max}$  where

$$b_{\min} = \frac{2}{Q} e^{-\gamma_E}, \quad b_{\max} = b_{\min} \exp \left( \frac{2\pi}{\beta_0 \alpha_s} \right), \quad (3.8)$$

and therefore we define

$$\mathcal{R}^{(\text{PT})}(b > b_{\max}) = \infty, \quad (3.9a)$$

$$\mathcal{R}^{(\text{PT})}(b < b_{\min}) = 0. \quad (3.9b)$$

From (2.16) we find the PT part of the  $q\bar{q}$  contribution within single logarithmic accuracy in the soft limit,

$$\mathcal{I}^{(\text{PT})}(t) \simeq \mathcal{I}_{q\bar{q}}^{(\text{PT})}(t) = \frac{Q^2}{2} \int bdb J_0(Qbt) e^{-\mathcal{R}^{(\text{PT})}(b)}. \quad (3.10)$$

We recall that the  $qg$  contribution does not contain single logarithmic PT terms. The matching of the approximate resummed expression (3.10) with the exact two-loop result will be dealt with in Section 5.1.

### 3.2 NP part of the radiator

The general expression (3.3) also contains an NP contribution. The latter is given by the non-analytic moments of  $\delta\alpha_{\text{eff}}$ , the NP component of the effective coupling (see Sect. 5.2). According to [9], the leading NP part of the radiator,  $\delta\mathcal{R}$ , is obtained from (3.3) by replacing  $\alpha_{\text{eff}}$  by  $\delta\alpha_{\text{eff}}$  and extracting from the rest of the integrand the leading term non-analytic in  $m^2$  at  $m^2 = 0$ . This term comes from the region  $\kappa_t^2 \sim m^2 \ll Q^2$  and therefore can be obtained by expanding the Bessel function in (3.3),

$$\begin{aligned} \delta\mathcal{R}(b) &= b^2 \cdot \frac{C_F}{4\pi} \int_0^\infty dm^2 \delta\alpha_{\text{eff}}(m) \frac{-d}{dm^2} \int_0^\infty \frac{\kappa_t^2 d\kappa_t^2}{m^2 + \kappa_t^2} \ln \frac{Q^2 e^{-\frac{3}{2}}}{m^2 + \kappa_t^2} \\ &= b^2 \cdot \frac{C_F}{2\pi} \int_0^\infty dm^2 \delta\alpha_{\text{eff}}(m) \ln^2 \frac{Qe^{-\frac{3}{4}}}{m} \equiv \frac{1}{2} b^2 \sigma. \end{aligned} \quad (3.11)$$

The upper limit in  $m^2$  is irrelevant here since  $\delta\alpha_{\text{eff}}$  has support at small  $m^2 \sim \Lambda_{\text{QCD}}^2$ . In the second line we have neglected terms which generate pieces analytic in  $m^2$ . The quantity  $\sigma$  contains two NP parameters,

$$\sigma \equiv -A_{2,1} \left( \ln Q^2 - \frac{3}{2} \right) + \frac{1}{2} A_{2,2} = \mathcal{A}_2 \left( \ln Q^2 - \frac{1}{2} \right) - \mathcal{A}'_2. \quad (3.12)$$

Here  $A$  and  $\mathcal{A}$  are the (log)moments of the NP effective coupling  $\delta\alpha_{\text{eff}}$  and of its dispersive companion  $\alpha_s^{\text{NP}}$ , respectively (see Sect. 5.2 below). From the relation between  $\sigma$  and the NP component of the running coupling,  $\alpha_s^{\text{NP}}$ ,

$$\sigma = \frac{C_F}{2\pi} \int_0^\infty dk^2 \left( \ln \frac{Q^2}{k^2} - \frac{1}{2} \right) \alpha_s^{\text{NP}}(k), \quad (3.13)$$

it is clear that the answer remains invariant under the choice of the scale of the logarithms in (3.12).

Taking account of the NP contribution to the radiator, the full quark-quark EEC is

$$\mathcal{I}_{q\bar{q}}(t) = \frac{Q^2}{2} \int bdb J_0(Qbt) e^{-\mathcal{R}^{(\text{PT})}(b)} e^{-\frac{1}{2} b^2 \sigma}. \quad (3.14)$$

The NP effect in the quark-antiquark correlation is nothing but a Gaussian smearing of the PT distribution  $\mathcal{I}^{(\text{PT})}(t)$ . Indeed, introducing a two-dimensional vector  $\vec{t}$  we can represent the answer in the form of a convolution

$$\mathcal{I}_{q\bar{q}}(t) = Q^2 \int d^2t' \frac{e^{-(\vec{t}-\vec{t}')^2 \frac{Q^2}{2\sigma}}}{2\pi \sigma} \mathcal{I}^{(\text{PT})}(t'), \quad (3.15)$$

with  $\mathcal{I}^{(\text{PT})}(t')$  the PT distribution given in (3.10).

Equation (3.15) makes it possible to directly relate the NP parameters entering into the definition of  $\sigma$  with observables describing soft hadronization. Even with PT radiation switched off, the direction of the leading quark undergoes a random walk in angle due to formation of the NP hadronic plateau. As a consequence we expect

$$\sigma = \langle k_{\perp}^2 \rangle \cdot n(Q), \quad n(Q) = \rho_h (\ln Q^2 - \Delta) \quad (3.16)$$

where  $\langle k_{\perp}^2 \rangle$  is the value of the mean squared transverse momentum of primary hadrons in jets,  $\rho_h$  is the density of the corresponding rapidity plateau and  $\Delta$  the parameter determining the effective length of the latter. This analogy gives

$$\mathcal{A}_2 = \langle k_{\perp}^2 \rangle \cdot \rho_h, \quad \mathcal{A}'_2 = \mathcal{A}_2 (\Delta - \frac{1}{2}). \quad (3.17)$$

A naive estimate of these numbers, ignoring the effects of resonance decays, may be obtained using the simplest exponential parametrization of the transverse momentum distribution of soft hadrons,

$$P(k_{\perp}) \propto k_{\perp} \exp(-2k_{\perp}/\langle k_{\perp} \rangle) \quad \langle k_{\perp} \rangle \simeq 0.30 - 0.35 \text{ GeV}, \quad (3.18)$$

together with the UA5 [16] parametrization of the charged multiplicity,

$$\bar{n}_{ch} = 9.11 s^{0.115} - 9.50 \simeq 1.05 \ln s - 0.39. \quad (3.19)$$

Taking account of neutrals, we find  $\rho_p \simeq 1.5$  and  $\Delta \simeq 0.4$ , while  $\langle k_{\perp}^2 \rangle = \frac{3}{2} \langle k_{\perp} \rangle^2 \simeq 0.13 - 0.18 \text{ GeV}^2$ , so that we may expect the NP parameters to be

$$\mathcal{A}_2 \simeq 0.20 - 0.27, \quad \mathcal{A}'_2 \simeq 0. \quad (3.20)$$

## 4. Quark-gluon correlation

The quark-gluon distribution  $\mathcal{I}_{qg}(t)$  can be expressed in terms of  $d\omega_1$  and  $d\omega_2$ , the one- and two-soft parton distributions which we have introduced for the radiator (see (3.1)). We have

$$\begin{aligned} \mathcal{I}_{qg}(t) = & \int \frac{d^2p d^2b}{(2\pi)^2} e^{i\vec{b}\vec{p}} e^{-\mathcal{R}(b)} \left\{ \int d\omega_1(k_1) u(k_1) e^{i\vec{b}\vec{\kappa}_{t1}} \right. \\ & \left. + \int d\omega_2(k_1 k_2) [u(k_1) + u(k_2)] e^{i\vec{b}(\vec{\kappa}_{t1} + \vec{\kappa}_{t2})} \right\}, \end{aligned} \quad (4.1)$$

where, according to (2.11), the functions  $u(k_i)$  which probe the EEC observable are

$$u(k_i) = 2\alpha_i \left[ \delta \left( t^2 - \frac{k_{t_i}^2}{Q^2 \alpha_i^2} \right) - \delta \left( t^2 - \frac{p^2}{Q^2} \right) \right]. \quad (4.2)$$

The relative transverse momentum  $\vec{\kappa}_{t_i}$  is defined in (2.6). The distribution  $d\omega_1$  is singular in the limit  $\alpha_1 \rightarrow 0$  as well as when the gluon momentum becomes parallel to that of the radiating quark,  $\vec{\kappa}_{t_1} \rightarrow 0$ . The first (infrared) singularity is compensated by the  $\alpha_1$  factor in  $u(k_1)$ . The collinear singularity cancels in the combination of delta functions in (4.2). A similar regularisation occurs in  $d\omega_2$  with respect to the “parent gluon” momentum. An additional (collinear) singularity in  $d\omega_2$  when the two offspring partons become parallel,  $\vec{\kappa}_{t_1}/\alpha_1 = \vec{\kappa}_{t_2}/\alpha_2$ , gets absorbed into the running coupling determining the emission of the parent gluon, see Appendix A.3.

#### 4.1 PT contribution

As shown in Appendix C.2, the PT component of  $\mathcal{I}_{qg}(t)$  constitutes a small  $\mathcal{O}(\alpha_s)$  relative correction to the “quark-quark” contribution

$$\mathcal{I}_{qg}^{(\text{PT})}(t) \sim \alpha_s(Q) \cdot \mathcal{I}_{q\bar{q}}^{(\text{PT})}(t).$$

In the first two orders in  $\alpha_s$  this contribution is fully taken into account by merging the approximate resummed expression with the exact  $\mathcal{O}(\alpha_s^2)$  result based on the matrix element calculation, as will be explained below in Section 5.1.

#### 4.2 NP contribution

Hereafter we concentrate on the NP component  $\mathcal{I}_{qg}^{(\text{NP})}$  of the quark-gluon correlation, which is the dominant power-behaved contribution to the EEC. Notice that the soft approximation which has been used to derive (4.1) suffices for this purpose.

Following the procedure introduced in [11], we compute in Appendix B the NP contribution and obtain

$$\mathcal{I}_{qg}^{(\text{NP})}(t) = \frac{C_F \mathcal{M}}{\pi} \int_0^\infty \frac{dm^2}{m^2} \delta\alpha_{\text{eff}}(m) \cdot \delta\Omega(m^2), \quad (4.3)$$

where the leading non-analytic piece of the trigger function is

$$\delta\Omega(m^2) = \frac{2m}{Q} \int \frac{d^2 t_g}{2\pi t_g^3} \left( \mathcal{I}_{q\bar{q}}(|\vec{t} - \vec{t}_g|) - \mathcal{I}_{q\bar{q}}(t) \right), \quad (4.4)$$

and  $\mathcal{M}$  the Milan factor. The NP contribution takes the form

$$\mathcal{I}_{qg}^{(\text{NP})}(t) = \frac{2\lambda}{Q} \int \frac{d^2 t_g}{2\pi t_g^3} \left( \mathcal{I}_{q\bar{q}}(|\vec{t} - \vec{t}_g|) - \mathcal{I}_{q\bar{q}}(t) \right), \quad (4.5)$$

with  $\mathcal{I}_{q\bar{q}}(t)$  the PT distribution given in (3.10). The NP parameter  $\lambda$  can be related to the first moment of the NP coupling defined Sect. 5.2 below:

$$\lambda = 2A_{1,0}\mathcal{M} = \frac{4}{\pi}\mathcal{A}_1\mathcal{M}. \quad (4.6)$$

Using (3.10) and the relation

$$\int \frac{d^2t_g}{2\pi t_g^3} \left( e^{i\vec{b}\vec{t}_g} - 1 \right) = -b, \quad (4.7)$$

the result can be expressed in terms of the mean value of the impact parameter  $b$  averaged over the quark distribution as follows:

$$\mathcal{I}_{qg}^{(\text{NP})}(t) = \frac{Q^2}{2} \int_0^\infty b db J_0(Qbt) e^{-\mathcal{R}(b)} (-2b\lambda). \quad (4.8)$$

Eq. (4.5) has a clear physical interpretation. It describes the contribution to the EEC when one triggers on a gluer (a gluon with  $\kappa_t \sim m \sim \Lambda$ ) in a given direction,  $\vec{t}$ , with respect to the thrust axis. The corresponding direction of the radiating quark is  $\vec{t}_p = \vec{t} - \vec{t}_g$ , where  $\vec{t}_g$  is the gluer direction with respect to the quark. This contribution is proportional to the gluer energy which, when expressed as the ratio  $\kappa_t/\theta$ , produces in Eqs. (4.4) and (4.5) an extra enhancement  $1/t_g$  on top of the standard logarithmic distribution  $d^2t_g/t_g^2$ . It is this additional singular factor which gives rise to the non-analytic contribution  $\sqrt{b^2}$  according to (4.7).

The convolution (4.5) remains finite due to “real-virtual” cancellation. The subtraction term represents the quark energy loss due to an unobserved gluer, which was disregarded in what we chose to call the quark-quark EEC distribution. Note that one consequence of this convenient subtraction convention is that what we call the quark-gluon contribution is not positive definite. We remark also that the structure of the NP quark-gluon contribution  $\mathcal{I}_{qg}$  does not suggest that it should be exponentiated.

Finally, observe that in the limit in which the accompanying radiation is neglected,  $\mathcal{R}(b) \rightarrow 0$ , one obtains

$$\mathcal{I}_{qg}^{(\text{NP})}(t) \rightarrow \frac{\lambda}{Q t^3}, \quad \frac{d\sigma^{(\text{NP})}}{\sigma d\cos\chi} \rightarrow \frac{2\lambda}{Q} \left( \frac{1+t^2}{2t} \right)^3 = \frac{2\lambda}{Q \sin^3\chi}, \quad (4.9)$$

which is the first order dispersive result, in accord with the NP expectation of [1].

By introducing the mean impact parameter  $\langle b \rangle = \langle b \rangle(t, Q)$  we can cast the NP  $qg$  contribution (4.8) as

$$\mathcal{I}_{qg}^{(\text{NP})}(t) = -2 \langle b \rangle \lambda \cdot \mathcal{I}_{q\bar{q}}(t). \quad (4.10)$$

For not too small values of  $t$ , such that  $\alpha_s \log^2 t < 1$ , we have  $\langle b \rangle \sim 1/(tQ)$ , which explains an additional  $1/t$  enhancement of the NP term on top of the kinematical

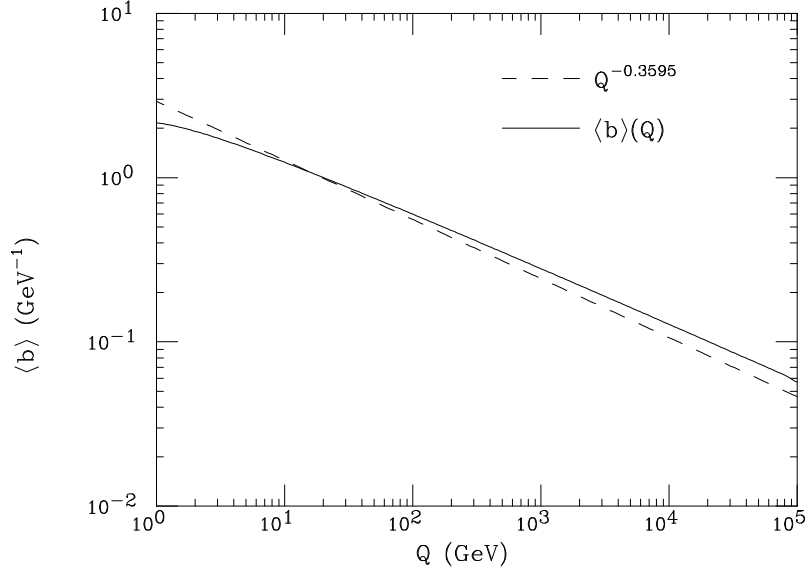


**Figure 1:** Quasi-linear dependence  $\log \langle b \rangle (0, Q)$  on  $\log Q$  with the expected slope

$1/t^2$  factor in (4.9). In the region  $\alpha_s \log^2 t > 1$  the Sudakov suppression effects slow down an increase of  $\langle b \rangle$  which flattens off and tends to a  $Q$ -dependent constant in the  $t \rightarrow 0$  limit.

If we use the one-loop coupling in the (two-loop) PT radiator, this behaviour can be explicitly computed (see Appendix D) to yield a non-integer exponent, see (D.22),

$$\langle b \rangle (0, Q) \simeq \frac{1.0894}{\Lambda_{\text{QCD}}} \left( \frac{\Lambda_{\text{QCD}}}{Q} \right)^{0.3236} \quad \text{for } n_f = 3, \quad \simeq \frac{1.1356}{\Lambda_{\text{QCD}}} \left( \frac{\Lambda_{\text{QCD}}}{Q} \right)^{0.3595} \quad \text{for } n_f = 5. \quad (4.11)$$

In Fig. 1 this analytical prediction for  $n_f = 5$ , shown by the dashed line, is compared with result of a numerical integration using the full two-loop perturbative radiator. The two-loop curve deviates only a little from the analytical one-loop calculation, which is reassuring.

The same hadronization model that was used in the previous Section to estimate the parameters  $\mathcal{A}_2$  and  $\mathcal{A}'_2$  gives for  $\mathcal{A}_1$  the value

$$\mathcal{A}_1 \mathcal{M} = \frac{\pi}{4} \rho_h \langle k_\perp \rangle \simeq 0.34 - 0.40 \text{ GeV}, \quad (4.12)$$

which follows from the comparison of the QCD and the “tube model” result for the leading power correction to the mean value of thrust, [17]

$$Q \langle 1 - T \rangle_{\text{NP}} = 2\lambda = 2\rho_h \langle k_\perp \rangle \simeq 1 \text{ GeV}. \quad (4.13)$$

## 5. Final results

Combining the  $q\bar{q}$  (2.10) and  $qg$  (4.8) contributions we obtain

$$\mathcal{I}(t) = \mathcal{I}_{q\bar{q}} + \mathcal{I}_{qg} = \frac{Q^2}{2} \int_0^\infty b db J_0(Qbt) e^{-\mathcal{R}^{(\text{PT})}(b) - \frac{1}{2}b^2\sigma} (1 - 2b\lambda) , \quad (5.1)$$

It should be clear that the NP  $qg$  correlation gives the dominant  $1/Q$  contribution, while the  $q\bar{q}$  effect, at the level of  $\log Q/Q^2$ , is much smaller, both formally and numerically. In particular, we did not consider the next-to-leading NP correction, potentially  $\mathcal{O}(Q^{-2})$ , coming from triggering  $qg$ . However, it should still be legitimate to keep at least the leading  $\log Q$ -enhanced piece in  $\sigma$ , provided the subleading  $1/Q^2$  correction from  $qg$  is not log-enhanced as well. To answer this question one would have to analyse  $\delta\Omega_{qg}$  further.

### 5.1 Matching resummed and fixed-order predictions

We consider the integrated EEC distribution

$$\Sigma(\chi) = \frac{1}{\sigma_{\text{tot}}} \int_0^\chi d\chi \frac{d\sigma}{d\chi} = \int_0^t \frac{4t dt}{(1+t^2)^2} \frac{d\Sigma}{d \cos \chi} \quad (5.2)$$

and use (1.2) to derive

$$\begin{aligned} \Sigma(\chi) &= C(\alpha_s) \frac{Q^2}{2} \int b db e^{-\mathcal{R}(b)} (1 - 2b\lambda) \int_0^t du u (1 + u^2) J_0(bQu) \\ &= C(\alpha_s) \frac{tQ}{2} \int db e^{-\mathcal{R}(b)} (1 - 2b\lambda) \left[ (1 + t^2) J_1(bQt) - \frac{2t}{bQ} J_2(bQt) \right]. \end{aligned} \quad (5.3)$$

Neglecting corrections of the order of  $t^2 \ll 1$  in the back-to-back region, we finally arrive at

$$\Sigma(\chi) = C(\alpha_s) \frac{tQ}{2} \int db J_1(bQt) e^{-\mathcal{R}(b)} (1 - 2b\lambda) + \mathcal{O}(t^2) . \quad (5.4)$$

We now take advantage of the existing exact two-loop PT prediction for EEC. To this end we write

$$\Sigma(\chi) = \Sigma_{\text{resum}}(\chi) + \delta\Sigma(\chi) \quad (5.5)$$

where  $\Sigma_{\text{resum}}$  is the resummed prediction, including NP corrections, and  $\delta\Sigma$  is the matching correction, which takes into account additional PT contributions up to  $\alpha_s^2$ .

In order to obtain sensible predictions at small  $\chi$ , we have to be careful to subtract and exponentiate *all* logarithmic terms up to this order, so that  $\delta\Sigma$  remains finite as  $\chi \rightarrow 0$ . The resummed expression based on the PT radiator accommodates



all logarithmically enhanced terms  $\alpha_s^n \log^m t$  with  $m \geq n$ . The finite non-logarithmic correction  $\mathcal{O}(\alpha_s)$  is taken care of in (5.4) by the one-loop coefficient function [6]

$$C(\alpha_s) = 1 - C_F \left( \frac{11}{2} + \frac{\pi^2}{3} \right) \frac{\alpha_s}{2\pi} \quad (5.6)$$

with  $\alpha_s = \alpha_s(Q)$  in the  $\overline{MS}$  renormalization scheme. At the  $\alpha_s^2$  level the first (and only) *singular* subleading logarithmic correction  $\mathcal{O}(\alpha_s^2 \log t)$  appears which has not been taken into account by the resummation procedure. We therefore include it into (5.4) to define

$$\Sigma_{\text{resum}}(\chi) = C(\alpha_s) \frac{tQ}{2} \exp \left[ -G_{21} \tau \left( \frac{\alpha_s}{2\pi} \right)^2 \right] \int_0^\infty db J_1(bQt) e^{-\mathcal{R}(b)} (1 - 2b\lambda), \quad (5.7)$$

where  $t = \tan(\chi/2)$  and  $\tau = \ln(1/t^2)$ . The coefficient  $G_{21}$  was obtained by fitting the single-logarithmic term in the two-loop PT contribution. In numerical evaluation of the integral in Eq. (5.7), the condition (3.9a) was imposed, so that impact parameters  $b > b_{\text{max}}$  do not contribute. We did not in fact impose the condition (3.9b) because its effect was found to be negligible.

The matching correction  $\delta\Sigma$  is then

$$\delta\Sigma(\chi) = \frac{1}{2} \left[ 1 + (A_1(\chi) - B_{11}\tau - B_{12}\tau^2) \frac{\alpha_s}{2\pi} + (A_2(\chi) - B_{21}\tau - B_{22}\tau^2 - B_{23}\tau^3 - B_{24}\tau^4) \left( \frac{\alpha_s}{2\pi} \right)^2 \right], \quad (5.8)$$

where  $A_1$  and  $A_2$  are the one- and two-loop predictions, obtained from the program EVENT2 [18], and the  $B_{ij}$ 's are the coefficients obtained by expanding Eq. (5.7) to second order in  $\alpha_s$ , which gives<sup>3</sup>

$$\begin{aligned} B_{11} &= 3C_F \\ B_{12} &= -C_F \\ B_{21} &= - \left( \frac{33}{2} + \pi^2 + 4\zeta(3) \right) C_F^2 + \left( \frac{67}{6} - \frac{\pi^2}{2} \right) C_F C_A - \frac{5}{3} C_F n_f - G_{21} \\ B_{22} &= \left( 10 + \frac{\pi^2}{3} \right) C_F^2 + \left( \frac{\pi^2}{6} - \frac{35}{36} \right) C_F C_A + \frac{1}{18} C_F n_f \\ B_{23} &= -3C_F^2 - \frac{11}{9} C_F C_A + \frac{2}{9} C_F n_f \\ B_{24} &= \frac{1}{2} C_F^2. \end{aligned}$$

Requiring  $\delta\Sigma(\chi)$  to be finite as  $\chi \rightarrow 0$  then gives  $G_{21} \simeq 65$ .

---

<sup>3</sup>Note that terms independent of  $\chi$  are irrelevant to the differential EEC and therefore we omit them.

## 5.2 Merging PT and NP contributions

Within the dispersive method the analysis of the perturbative and non-perturbative contribution is performed by splitting the coupling into two parts

$$\alpha_s(k) = \alpha_s^{\text{PT}}(k) + \alpha_s^{\text{NP}}(k), \quad (5.9a)$$

$$\alpha_{\text{eff}}(m) = \alpha_{\text{eff}}^{\text{PT}}(m) + \delta\alpha_{\text{eff}}(m). \quad (5.9b)$$

It is assumed that  $\alpha_s^{\text{NP}}(k)$  has a finite support, that is, it decreases fast at large  $k^2$ . This implies that  $\alpha_{\text{eff}}(m)$  has only non-analytic  $m^2$  moments,

$$A_{2p,q} = \frac{C_F}{2\pi} \int \frac{dm^2}{m^2} \delta\alpha_{\text{eff}}(m) (m^2)^p \ln^q m^2, \quad (5.10)$$

with  $p$  non-integer or  $q \neq 0$ . Using (3.2) it is straightforward to relate these parameters to the moments of  $\alpha_s^{\text{NP}}(k)$ ,

$$\begin{aligned} \mathcal{A}_{2p} &= \frac{C_F}{2\pi} \int \frac{dk^2}{k^2} (k^2)^p \alpha_s^{\text{NP}}(k), \\ \mathcal{A}'_{2p} &= \frac{d}{dp} \mathcal{A}_{2p} = \frac{C_F}{2\pi} \int \frac{dk^2}{k^2} (k^2)^p \ln k^2 \alpha_s^{\text{NP}}(k), \end{aligned} \quad (5.11)$$

as follows [19]

$$A_{2p,q} = \frac{d^q}{dp^q} \left[ \frac{\sin \pi p}{\pi p} \mathcal{A}_{2p} \right]. \quad (5.12)$$

In particular one has

$$A_{1,0} = \frac{2}{\pi} \mathcal{A}_1, \quad A_{2,1} = -\mathcal{A}_2, \quad A_{2,2} = -2\mathcal{A}'_2 + 2\mathcal{A}_2. \quad (5.13)$$

In order to define these parameters more precisely, the problem of merging the perturbative and non-perturbative contributions must be addressed. The relevant procedure was discussed in detail in [20]. It involves introducing an infrared matching scale  $\mu_1$  (typically chosen to be  $\mu_1 = 2$  GeV), above which the NP component of  $\alpha_s$  is assumed to be negligible. The PT prediction for a given observable contains a contribution from the region  $\mu < \mu_1$ . If it is calculated to next-to-leading order, then the PT coupling is represented by its two-loop expansion with respect to  $\alpha_s \equiv \alpha_{\overline{\text{MS}}}(Q)$ :

$$\alpha_s^{\text{PT}}(k) = \alpha_s + \frac{\beta_0}{2\pi} \left( \ln \frac{Q}{k} + \frac{K}{\beta_0} \right) \alpha_s^2. \quad (5.14)$$

The term proportional to  $K$  accounts for mismatch between the  $\overline{\text{MS}}$  and bremsstrahlung renormalization schemes, with  $K$  given below in (C.9).

Defining the moments of the coupling on the interval  $0 < k < \mu_1$ , normalized in such a way that they would all be equal if  $\alpha_s(k)$  were constant in this region,

$$\bar{\alpha}_{p,q}(\mu_1) \equiv \frac{(p+1)^{q+1}}{q! \mu_1^{p+1}} \int_0^{\mu_1} dk k^p \ln^q \frac{\mu_1}{k} \alpha_s(k), \quad (5.15)$$

we have

$$\bar{\alpha}_{p,q}^{\text{PT}}(\mu_1) = \alpha_s + \frac{\beta_0}{2\pi} \left( \ln \frac{Q}{\mu_1} + \frac{K}{\beta_0} + \frac{q+1}{p+1} \right) \alpha_s^2. \quad (5.16)$$

By subtraction, we can now express the non-perturbative parameters (5.11) in terms of the full moments (5.15). In particular we have

$$\begin{aligned} \mathcal{A}_{2p} &= \mu_1^{2p} \cdot \frac{C_F}{2\pi p} [\bar{\alpha}_{2p-1}(\mu_1) - \bar{\alpha}_{2p-1}^{\text{PT}}(\mu_1)] , \\ \mathcal{A}'_{2p} &= \mu_1^{2p} \cdot \frac{C_F}{2\pi p^2} \{ p \ln \mu_1^2 [\bar{\alpha}_{2p-1}(\mu_1) - \bar{\alpha}_{2p-1}^{\text{PT}}(\mu_1)] - \bar{\alpha}_{2p-1,1}(\mu_1) + \bar{\alpha}_{2p-1,1}^{\text{PT}}(\mu_1) \} , \end{aligned} \quad (5.17)$$

where  $\bar{\alpha}_{2p-1} \equiv \bar{\alpha}_{2p-1,0}$ . Note that these quantities depend, via (5.14), on the order of perturbation theory used to make the PT prediction. If this is extended to next-to-next-to-leading order then a further term of order  $\alpha_s^3$ , which can easily be computed, should be added to (5.14). The corresponding PT terms in (5.16), which diverge factorially in higher orders, represent the start of the series responsible for subtracting off the infrared renormalon divergence in the *perturbative* contribution to the observable. Thus there is no renormalon ambiguity in the sum of the PT and NP contributions.

The NP parameters  $\lambda$  and  $\sigma$  introduced above are now given by

$$\lambda = \mathcal{M} \frac{4C_F}{\pi^2} \mu_1 [\bar{\alpha}_0(\mu_1) - \bar{\alpha}_0^{\text{PT}}(\mu_1)] , \quad (5.18a)$$

$$\sigma = \frac{C_F}{2\pi} \mu_1^2 \left\{ \left( \ln \frac{Q^2}{\mu_1^2} - \frac{1}{2} \right) [\bar{\alpha}_1(\mu_1) - \bar{\alpha}_1^{\text{PT}}(\mu_1)] + \bar{\alpha}_{1,1}(\mu_1) - \bar{\alpha}_{1,1}^{\text{PT}}(\mu_1) \right\} . \quad (5.18b)$$

Here  $\mathcal{M}$  in (5.18a) is the Milan factor resulting from the two-loop analysis discussed in Appendix B (see also [11]). This factor is universal for all  $1/Q$  jet observables considered in  $e^+e^-$  annihilation [20] and DIS processes [21] and reads

$$\mathcal{M} = 1 + \beta_0^{-1} (2.437C_A - 0.052n_f) = 1.920 (1.665) \quad \text{for } n_f = 5 (0) . \quad (5.19)$$

## 6. Comparison with experiment

In this section we compare the above predictions with experimental data on the EEC near the backward direction. At present the data are not plentiful and are not usually binned in the optimal way for such comparisons. Therefore, rather than attempting a detailed fit, we used “default” values of the relevant parameters. The only perturbative parameter is the QCD scale, which we fixed to be<sup>4</sup>

$$\Lambda_{\overline{\text{MS}}}^{(n_f=5)} = 0.23 \text{ GeV} , \quad (6.1)$$

---

<sup>4</sup>We consistently used  $n_f = 5$  in the calculation of the radiator and the matching correction  $\delta\Sigma$ , as well as in the Milan factor where it appears more questionable.

which corresponds to  $\alpha_s(M_Z) = 0.118$ . The three non-perturbative parameters are moments of the coupling  $\alpha_s(k)$  over the infrared region  $0 < k < \mu_I$ , which enter into Eqs. (5.18) and are defined by (5.15). Choosing  $\mu_I = 2$  GeV, for the first two we take the values

$$\bar{\alpha}_0(2 \text{ GeV}) = 0.50, \quad \bar{\alpha}_1(2 \text{ GeV}) = 0.45, \quad (6.2)$$

which come from analyses of  $1/Q$  effects in event shapes [8,22] and  $1/Q^2$  corrections to deep inelastic structure functions [23], respectively. For the second log-moment, a new parameter which has not been probed in other observables, we take the value according to the model of Ref. [24], which is also consistent with the values (6.2):

$$\bar{\alpha}_{1,1}(2 \text{ GeV}) = 0.55. \quad (6.3)$$

In terms of the dimensionful parameters defined in (5.11), these values correspond to

$$\mathcal{A}_1 \mathcal{M} \simeq 0.33 \text{ GeV}, \quad \mathcal{A}_2 \simeq 0.2 \text{ GeV}^2, \quad \mathcal{A}'_2 \simeq 0.0 \text{ GeV}^2 \quad (6.4)$$

at  $Q \sim M_Z$ . Owing to the residual  $Q$ -dependence in Eq. (5.16),  $\mathcal{A}_1$  and  $\mathcal{A}_2$  are somewhat reduced at lower energies (falling to 0.2 and 0.12 respectively at  $Q \simeq 10$  GeV), while  $\mathcal{A}'_2$  remains consistent with zero.

The theoretical predictions are compared with data on the distribution in the angle  $\chi = \pi - \theta$  at a range of energies in Figs. 2 and 3. The dot-dashed curves show the second-order PT predictions, while the long-dashed curves display the results of purely perturbative resummation. The short-dashed curves include the NP quark-antiquark smearing effects, and the final results including the NP quark-gluon correlation are shown by the solid curves.

The effect of PT resummation is to dramatically reduce the cross section at small  $\chi$ , i.e. for nearly back-to-back kinematics [3–5], but not enough to match the data. The NP contributions give a further reduction at small  $\chi$  and an enhancement at larger values. For  $Q \sim M_Z$  the NP effects are dominated by the quark-gluon contribution linear in  $b$ , while the quadratic NP contributions to the radiator, due to quark-antiquark smearing, become important at lower energies.

The distribution in  $\chi$  has a kinematical suppression of the most interesting region of small angles. The distribution in  $\cos \chi$ , which is finite at  $\chi = 0$ , is more informative. Regrettably the only data set we could find that is binned in this way is at the single energy  $Q \simeq 30$  GeV [25]. A comparison with the theoretical expectations, again using the default parameters given above, is shown in Fig. 4.

All the predicted distributions are in reasonable agreement with the experimental data. We would like to stress, however, that the  $\cos \theta$  distribution is much more sensitive to the NP effects. With more precise data binned in  $\cos \theta$  over a wide range of energies, it should be possible to attempt quantitative fits to extract the values of the important NP parameters, including the new quantity  $\bar{\alpha}_{1,1}$ .

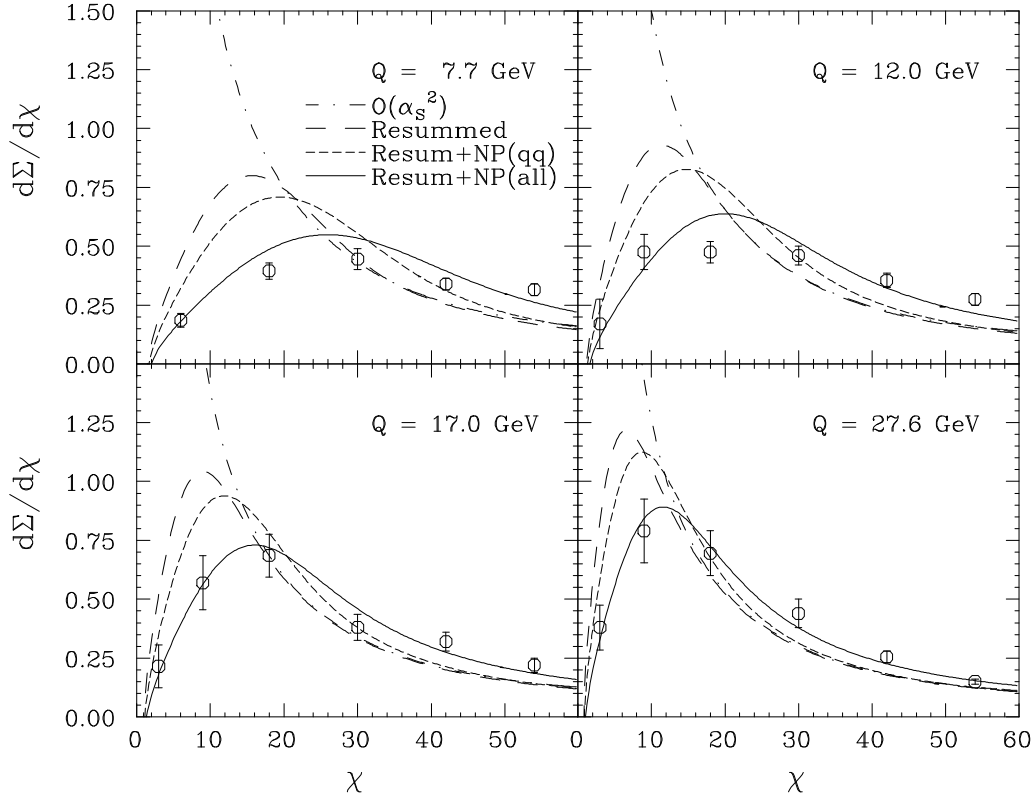


**Figure 2:** PLUTO [25] data on the  $\chi$  distribution of the EEC, compared with PT and NP predictions.

## 7. Discussion

In this paper we have investigated the leading power-behaved non-perturbative contributions to the EEC. In particular we have demonstrated that the power-suppressed contributions to the EEC distribution in the back-to-back region are strongly modified by the interplay with purely perturbative multiparton emission effects. Thus the expected  $1/Q$  behaviour of the leading non-perturbative term due to the quark-gluon correlation turns into<sup>5</sup>  $(1/Q)^{0.32-0.36}$ , while the  $Q$ -dependence of the contribution due to NP smearing effects in the quark-quark EEC,  $\log Q/Q^2$ , slows down to  $(1/Q)^{0.58-0.65}$ . The latter effect should also be present in the differential transverse momentum distribution of massive Drell-Yan lepton pairs in hadron-hadron collisions, at small transverse momenta,  $p_{\perp} \ll M$ . Since the Drell-Yan process is fully inclusive with respect to gluons, the “ $1/Q$ ” effect which was leading in the EEC case should be absent from the transverse momentum distribution, as it is from the integrated cross section [9, 28].

<sup>5</sup>The values of the exponents we present here correspond to  $n_f = 3$  and 5, respectively. These estimates are based on an analytical treatment using the one-loop coupling. The actual two-loop exponent of the quark-gluon contribution, in particular, is even smaller at achievable energies, see Fig. 1.

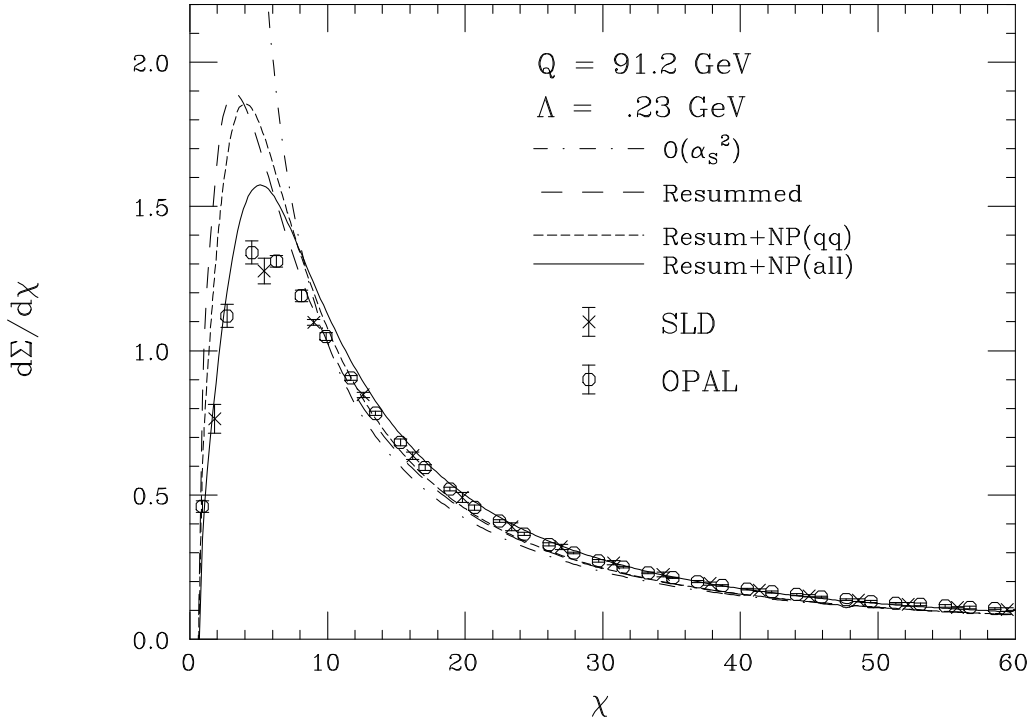


**Figure 3:** SLD [26] and OPAL [27] data on the  $\chi$  distribution of the EEC, compared with PT and NP predictions.

At the perturbative level, the present analysis includes the fully resummed next-to-leading logarithmic expression for the EEC distribution based on the two-loop radiator, which has been matched with the exact order  $\alpha_s^2$  result provided by EVENT2 [18].

As far as non-perturbative physics is concerned, the aim of this paper was to demonstrate consistency with the general framework provided by the dispersive approach and with the concept of universality of confinement effects. Therefore we have not attempted a detailed quantitative analysis but rather have compared with expectations based on other processes.

The leading NP effects are controlled by three phenomenological parameters. The most important of them, which determines the NP  $qg$  contribution, is the one that describes  $1/Q$  contributions to the means and distributions of various jet shapes. The value of this parameter,  $\bar{\alpha}_0(2 \text{ GeV}) \simeq 0.50$ , we have taken from jet shape phenomenology.

The other two parameters,  $\bar{\alpha}_1$  and  $\bar{\alpha}_{1,1}$ , determine the  $\log Q$ -enhanced and the constant terms of the NP “ $1/Q^2$ ”  $q\bar{q}$  contribution respectively. The first of the two,  $\bar{\alpha}_1(2 \text{ GeV}) \simeq 0.45$ , we have taken from the analysis of power corrections to the DIS structure functions. Finally, the log-moment  $\bar{\alpha}_{1,1}(2 \text{ GeV}) \simeq 0.55$  we have borrowed from the model of Ref. [24], since it is a new quantity which has not yet been probed in other processes.



the assumption of Collins and Soper, our approach does not suggest that such linear terms should be exponentiated.

The dispersive approach also gives rise naturally to contributions that are quadratic in  $b$  (and  $\log Q$  enhanced), which can be interpreted as a NP smearing of the quark-antiquark correlation. Collins and Soper's parametrization allowed for such contributions but they were not included in their comparisons with experiment. In our treatment the linear and quadratic contributions are comparable at low energies, with the former becoming dominant at  $Q \sim M_Z$ . This emphasises again the importance of comprehensive experimental studies over the widest possible range of energies.

## Acknowledgements

This research was supported in part by the EU Fourth Framework Programme 'Training and Mobility of Researchers', Network 'Quantum Chromodynamics and the Deep Structure of Elementary Particles', contract FMRX-CT98-0194 (DG 12 - MIHT). GM and BRW are grateful for the hospitality of the CERN Theory Division during a part of this work. We benefited from discussions with G.P. Korchemsky, G.P. Salam and D.E. Soper.

## A. Radiator

### A.1 Phase space and momentum balance

In terms of Sudakov variables, the phase space for the emission of the primary quark-antiquark pair together with  $n$  partons

$$d\Phi_n = (2\pi)^4 \delta^4 \left( p + \bar{p} + \sum_i k_i - Q \right) \frac{d^4 p}{(2\pi)^3} \delta(p^2) \frac{d^4 \bar{p}}{(2\pi)^3} \delta(\bar{p}^2) \prod_i \frac{d^4 k_i}{(2\pi)^3} \delta(k_i^2), \quad (\text{A.1})$$

can be written as

$$d\Phi_n = \frac{d\Omega}{4\pi} \zeta \frac{d\rho}{\rho} d^2 p_t \delta^2(\vec{p}_t + \sum_i \vec{k}_{ti}) \delta(1 - \rho - \sum_i \alpha_i) \prod_i \frac{d\alpha_i}{\alpha_i} \frac{d^2 k_{ti}}{2(2\pi)^3}. \quad (\text{A.2})$$

Introducing parton transverse momenta with respect to the antiquark direction,  $\vec{\kappa}_{ti}$  (2.6), and the angular antiquark variable  $\vec{p}$  defined in (2.12), we can write

$$d\Phi_n = \frac{d\Omega}{4\pi} d^2 p \delta^2(\vec{p} + \sum_i \vec{\kappa}_{ti}) \zeta \rho \prod_i \frac{d\alpha_i}{\alpha_i} \frac{d^2 \kappa_{ti}}{2(2\pi)^3}, \quad (\text{A.3})$$

with

$$\zeta = 1 - \sigma - \sum_i \beta_i, \quad \rho = 1 - \sum_i \alpha_i, \quad \sigma = \rho \frac{p^2}{Q^2}.$$



Since the soft matrix elements are factorized it is convenient to express also the phase space in a factorized form. This is obtained by introducing the impact parameter  $\vec{b}$  to represent the transverse momentum conservation

$$d\Phi_n = \frac{d\Omega}{4\pi} d^2p \int \frac{d^2b}{(2\pi)^2} e^{i\vec{b}\vec{p}} \zeta \rho \prod_i \frac{d\alpha_i}{\alpha_i} \frac{d^2\kappa_{ti}}{2(2\pi)^3} e^{i\vec{b}\vec{\kappa}_{ti}}. \quad (\text{A.4})$$

In the soft limit the upper bounds of the parton momentum integrations can be arbitrarily chosen as  $\kappa_{ti} < Q$  and  $\alpha_i < 1$ . An improper treatment of the hard region of the phase space is then corrected by introducing the coefficient function factor  $C(\alpha_s)$  (see (2.8)) and performing the matching of the approximate resummed expression with the exact matrix element calculation to the two-loop order, which was discussed in detail in Section 5.1.

We will say that a secondary parton with

$$\alpha_i > \beta_i = \frac{k_{ti}^2}{\alpha_i Q^2}, \quad \text{or} \quad \beta_i > \alpha_i = \frac{k_{ti}^2}{\beta_i Q^2},$$

is emitted in the *right*- or *left*-hemisphere respectively. (Within this convention the quark belongs to the left hemisphere.) We have chosen the Sudakov representation based on the *quark* momentum direction. Therefore, as long as the quark and antiquark are generally not back-to-back, the invariant phase space is not symmetric with respect to left-right exchanges.

However, (A.4) remains symmetric with respect to the R–L hemispheres at the level of the terms *linear* in gluon momenta, which approximation is sufficient both for deriving the resummed PT distribution and for extracting the leading NP effects. Indeed, to this accuracy we may write

$$\rho \zeta = \left(1 - \sum_{i=1}^n \alpha_i\right) \left(1 - \sum_{i=1}^n \beta_i - \sigma\right) \approx \prod_{i=1}^n (1 - \alpha_i) (1 - \beta_i), \quad (\text{A.5})$$

where we have neglected the quadratic terms  $\mathcal{O}(\alpha_i \alpha_j)$  in the first factor and both  $\mathcal{O}(\beta_i \beta_j)$  and  $\sigma \propto p_i^2$  in the second factor. In conclusion, in the soft limit including quark recoil, we may use

$$\zeta \rho \prod_i \frac{d\alpha_i}{\alpha_i} \simeq \prod_i \left[ d\alpha_i \frac{1 - \alpha_i}{\alpha_i} \vartheta(\alpha_i Q - k_{ti}) + d\beta_i \frac{1 - \beta_i}{\beta_i} \vartheta(\beta_i Q - k_{ti}) \right]. \quad (\text{A.6})$$

Here we have split the radiation into two hemispheres. For the emission in the right hemisphere,  $\alpha_i > \beta_i$ , we included the factor  $(1 - \alpha_i)$  from (A.5), and similarly the factor  $(1 - \beta_i)$  for the emission in the left hemisphere.

## A.2 One-loop radiator

The soft multi-gluon radiation probability at one loop (multiple independent soft gluon emission) takes the form

$$dw_n = d\Phi_n |M_n|^2 \simeq d^2p \int \frac{d^2b}{(2\pi)^2} e^{i\vec{b}\vec{p}} \times \frac{1}{n!} \prod_i \left\{ \frac{C_F \alpha_s}{\pi} \frac{d^2\kappa_{ti}}{\pi \kappa_{ti}^2} e^{i\vec{b}\vec{\kappa}_{ti}} \left[ d\alpha_i \frac{1-\alpha_i}{\alpha_i} \vartheta(\alpha_i Q - \kappa_{ti}) + d\beta_i \frac{1-\beta_i}{\beta_i} \vartheta(\beta_i Q - \kappa_{ti}) \right] \right\}, \quad (\text{A.7})$$

where we have expressed the phase space for the emission in the right and left hemisphere in terms of  $\alpha_i$  and  $\beta_i$  respectively. Here we have substituted  $\kappa_t$  for  $k_t$  in the theta-functions determining the Right-Left hemispheres. This pretty voluntary action is safe: the mismatch between the lower limits of the  $\alpha$ -integration expressed in terms of the transverse momentum defined with respect the quark,  $k_t$ , and the antiquark,  $\kappa_t$ , is relatively small for small  $k_t$  and/or small  $p_t$ , which is our region of interest.

The factor  $(1-\alpha)/\alpha$  is the classical part of gluon emission which, according to the celebrated Low-Barnett-Kroll theorem [29] embodies both the soft singularity,  $d\alpha/\alpha$ , and the first linear correction,  $d\alpha \cdot \mathcal{O}(1)$ . Taking account of the true hard gluon radiation,  $\frac{1}{2}\alpha d\alpha$ , this factor gets promoted to the full quark-gluon splitting function  $P(\alpha)$ ,

$$\frac{1-\alpha}{\alpha} \implies P(\alpha) = \frac{1+(1-\alpha)^2}{2\alpha}.$$

Introducing the standard subtraction to accommodate virtual contributions we arrive at the  $n$ -gluon emission probability,

$$dw_n = d^2p \int \frac{d^2b}{(2\pi)^2} e^{i\vec{b}\vec{p}} dW_n, \quad (\text{A.8})$$

where  $dW_n$  factorizes (for given  $\vec{b}$  and  $p \ll 1$ ) into  $n_R$  and  $n_L$  soft gluons emitted into the right- and left-hemispheres,

$$dW_n = dW_{n_R} \cdot dW_{n_L}, \quad n = n_R + n_L. \quad (\text{A.9})$$

Each of the two distributions is given by the soft factorized expression. The right-hemisphere distribution reads

$$dW_{n_R} = \exp \left\{ -\frac{C_F \alpha_s}{\pi} \int_0^1 d\alpha P(\alpha) \int_0^{Q^2} \frac{d\kappa_t^2}{\kappa_t^2} \vartheta(\alpha Q - \kappa_t) \right\} \times \frac{1}{n_R!} \prod_{i=1}^{n_R} \left\{ \frac{C_F \alpha_s}{\pi} d\alpha_i P(\alpha_i) \frac{d\kappa_{ti}^2 \vartheta(\alpha_i Q - \kappa_{ti})}{\kappa_{ti}^2} J_0(b\kappa_{ti}) \right\}. \quad (\text{A.10})$$

A similar expression holds for the left-hemisphere contribution. Summing over  $n$  and integrating  $dW_n$  one obtains

$$\sum_n \int dW_n = e^{-\mathcal{R}(b)}, \quad (\text{A.11})$$

where  $\mathcal{R}(b)$  is the one-loop radiator which receives contributions from the radiation into both hemispheres. It is given by (see (A.10))

$$\begin{aligned} \mathcal{R}(b) &= \int_0^1 d\alpha \frac{C_F \alpha_s}{\pi} P(\alpha) \int_0^{Q^2} \frac{d\kappa_t^2}{\kappa_t^2} [1 - J_0(b\kappa_t)] 2 \cdot \vartheta(\alpha Q - \kappa_t) \\ &\simeq \int_0^{Q^2} \frac{d\kappa_t^2}{\kappa_t^2} \frac{C_F \alpha_s}{\pi} [1 - J_0(b\kappa_t)] \ln \frac{Q^2 e^{-3/2}}{\kappa_t^2}, \end{aligned} \quad (\text{A.12})$$

where the factor 2 in front of the theta function accounts for the two hemispheres. We have  $\mathcal{R}(0) = 0$  which ensures the expected normalization to the total cross section,

$$\sum_n \int dw_n(k_1 \cdots k_n, \vec{b}) = \int \frac{d^2 p d^2 b}{(2\pi)^2} e^{i\vec{b}\vec{p}} e^{-\mathcal{R}(b)} = 1. \quad (\text{A.13})$$

### A.3 Two-loop radiator

We now consider the two-loop improvement. By using the results of [11] we can generalise the form of the one-loop radiator to include two-loop corrections in the soft region. The radiator is given by (3.1) where the one and two uncorrelated soft parton distributions  $d\omega_1$  and  $d\omega_2$  are given by

$$d\omega_1(k) \equiv 4C_F d\alpha P(\alpha) \frac{d\kappa_t^2}{\kappa_t^2} 2\vartheta(\alpha Q - \kappa_t) \left\{ \frac{\alpha_s(0)}{4\pi} + \chi(\kappa_t) \right\}, \quad (\text{A.14a})$$

$$d\omega_2(k_1 k_2) \equiv 4C_F d\Gamma_2(k_1, k_2) \left( \frac{\alpha_s}{4\pi} \right)^2 \frac{1}{2!} M^2(k_1, k_2). \quad (\text{A.14b})$$

We briefly recall here the structure of these distributions [11].

The first distribution  $d\omega_1$  describes emission of a single real gluon, with  $\alpha_s(0)$  its on-shell coupling and  $\chi(\kappa_t)$  the one-loop virtual vertex correction given by

$$\frac{\chi(\kappa_t)}{\kappa_t^2} = \int_0^{Q^2} \frac{d\mu^2}{\mu^2(\mu^2 + \kappa_t^2)} \left( \frac{\alpha_s}{4\pi} \right)^2 \left\{ -2C_A \ln \frac{\kappa_t^2(\kappa_t^2 + \mu^2)}{\mu^4} \right\}. \quad (\text{A.15})$$

The dispersive representation (A.15) determines  $\chi(\kappa_t)$  up to a scheme-dependent constant, of order  $\alpha_s^2$ . Setting this constant to zero, corresponds to the choice of the bremsstrahlung scheme [14]. In (A.15) we have chosen to set the ultraviolet integration limit at  $\mu^2 = Q^2$ , rather than  $\mu^2 = \infty$ , in order to have the exact inclusive cancellation with the real emission. The error,  $\mathcal{O}(\alpha_s)$ , induced by such a choice is compensated by fixing the coefficient function appropriately. The theta function in

(A.14a) selects the gluons emitted in the right-hemisphere; the accompanying factor of 2 takes care of the contribution from the opposite (quark) hemisphere.

The distribution  $d\omega_2(k_1 k_2)$  given in (A.14b) corresponds to the emission of two soft partons with 4-momenta  $k_1$  and  $k_2$ . The uncorrelated ‘‘Abelian’’ two-gluon emission being subtracted off, the rest can be described as the contribution from the radiation of a (virtual) gluon followed by its decay into  $q\bar{q}$  or  $gg$  in the final state. The corresponding matrix element  $M$  can be found in [11]. The two-parton phase space  $d\Gamma_2$  reads

$$d\Gamma_2 = dm^2 \frac{d\alpha}{\alpha} \frac{d^2\kappa_t}{\pi} \cdot dz \frac{d\phi}{2\pi},$$

where  $\alpha = \alpha_1 + \alpha_2$ ,  $\vec{\kappa}_t = \vec{\kappa}_{t1} + \vec{\kappa}_{t2}$  and  $m^2 = (k_1 + k_2)^2$  are the ‘‘parent gluon’’ variables, while  $z$  and  $\phi$  are the momentum fraction and relative azimuth of the two secondary partons,  $q\bar{q}$  or  $gg$ . The following kinematical relations hold:

$$\alpha_1 = z\alpha, \quad \alpha_2 = (1-z)\alpha; \quad \vec{q}_t = \frac{\vec{\kappa}_{t1}}{z} - \frac{\vec{\kappa}_{t2}}{1-z}; \quad m^2 = z(1-z)q_t^2. \quad (\text{A.16})$$

Integrating  $M^2$  over  $z$  and  $\phi$  one finds [11]

$$\int dz \frac{d\phi}{2\pi} \frac{1}{2!} M^2(k_1, k_2) = \frac{1}{m^2(m^2 + k_t^2)} \left( \frac{\alpha_s}{4\pi} \right)^2 \left\{ 2C_A \ln \frac{k_t^2(k_t^2 + m^2)}{m^4} - \beta_0 \right\}, \quad (\text{A.17})$$

with  $\beta_0$  the one-loop coefficient of the beta function.

Performing the  $\alpha$ -integration (over both hemispheres) of the radiator  $\mathcal{R}(b)$  given in (3.1) we arrive at

$$\begin{aligned} \mathcal{R}(b) &= 4C_F \int_0^{Q^2} \frac{d\kappa_t^2}{\kappa_t^2} \ln \frac{Q^2 e^{-\frac{3}{2}}}{\kappa_t^2} \left( \frac{\alpha_s(0)}{4\pi} + \chi(\kappa_t) \right) [1 - J_0(b\kappa_t)] \\ &+ 4C_F \int_0^{Q^2} \frac{dm^2}{m^2} \left( \frac{\alpha_s}{4\pi} \right)^2 \int_0^{Q^2} \frac{d\kappa_t^2}{\kappa_t^2 + m^2} \ln \frac{Q^2 e^{-\frac{3}{2}}}{\kappa_t^2 + m^2} \left\{ 2C_A \ln \frac{\kappa_t^2(\kappa_t^2 + m^2)}{m^4} - \beta_0 \right\} [1 - J_0(b\kappa_t)]. \end{aligned} \quad (\text{A.18})$$

The collinear divergent terms, namely the logarithmic term on the second line and the virtual contribution  $\chi(\kappa_t)$ , cancel if we neglect the mismatch between the real and virtual phase space, which is proportional to the factor  $\ln(\kappa_t^2/(\kappa_t^2 + m^2))$ . This mismatch vanishes as  $m^2/\kappa_t^2$  for  $m^2 \ll \kappa_t^2$  and, as we shall see later, proves to be negligible within our accuracy both for the PT and NP part of the radiator.

We are left then with the regular contribution proportional to  $\beta_0$ , and we get

$$\begin{aligned} \mathcal{R}(b) &= 4C_F \int_0^{Q^2} dm^2 \left\{ \frac{\alpha_s(0)}{4\pi} \delta(m^2) - \frac{\beta_0}{m^2} \left( \frac{\alpha_s}{4\pi} \right)^2 \right\} \\ &\times \int_0^{Q^2} \frac{d\kappa_t^2}{\kappa_t^2 + m^2} \ln \frac{Q^2 e^{-\frac{3}{2}}}{\kappa_t^2 + m^2} [1 - J_0(b\kappa_t)]. \end{aligned} \quad (\text{A.19})$$

The two contributions in the curly brackets in (A.19) combine to produce the running coupling. To see this we invoke the dispersive representation (3.2) for  $\alpha_s$  in terms of the effective coupling  $\alpha_{\text{eff}}$ , which gives, under the  $m^2$  integral,

$$\left\{ \frac{\alpha_s(0)}{4\pi} \delta(m^2) - \frac{\beta_0}{m^2} \left( \frac{\alpha_s}{4\pi} \right)^2 + \mathcal{O}(\alpha_s^3) \right\} \cdot = \frac{\alpha_{\text{eff}}(m)}{4\pi} \left( \frac{-d}{dm^2} \right). \quad (\text{A.20})$$

This leads to the following representation for the two-loop radiator (A.19):

$$\begin{aligned} \mathcal{R}(b) &= \frac{C_F}{\pi} \int_0^{Q^2} dm^2 \alpha_{\text{eff}}(m) \frac{-d}{dm^2} \int_0^{Q^2} \frac{d\kappa_t^2}{m^2 + \kappa_t^2} [1 - J_0(b\kappa_t)] \ln \frac{Q^2 e^{-\frac{3}{2}}}{m^2 + \kappa_t^2} \\ &= \frac{C_F}{\pi} \int_0^{Q^2} dm^2 \alpha_{\text{eff}}(m) \int_0^{Q^2} \frac{d\kappa_t^2}{(m^2 + \kappa_t^2)^2} [1 - J_0(b\kappa_t)] \left( \ln \frac{Q^2 e^{-\frac{3}{2}}}{m^2 + \kappa_t^2} + 1 \right). \end{aligned} \quad (\text{A.21})$$

**Perturbative equivalence.** Within single logarithmic accuracy (A.21) is perturbatively equivalent to the well known expression

$$\mathcal{R}(b) = \frac{C_F}{\pi} \int_0^{Q^2} \frac{d\kappa_t^2}{\kappa_t^2} \alpha_s(\kappa_t) [1 - J_0(b\kappa_t)] \ln \frac{Q^2 e^{-\frac{3}{2}}}{\kappa_t^2}, \quad (\text{A.22})$$

with  $\alpha_s$  taken in the bremsstrahlung scheme [14].

To show that (A.21) and (A.22) coincide at two-loop level, we first extend the  $m^2$ -integration in (A.21) to infinity. This produces a correction of the relative order  $\alpha_s(Q) \cdot k_t^2/Q^2$  which gives rise to a non-logarithmic correction to  $\mathcal{R}$  of the order  $\mathcal{O}(\alpha_s(Q))$ , which we drop as belonging to the coefficient function. Then from the dispersive relation (3.2) one finds

$$\begin{aligned} \int_0^\infty \frac{dm^2 \alpha_{\text{eff}}(m)}{(m^2 + k_t^2)^2} \left[ \ln \frac{Q^2 e^{-\frac{3}{2}}}{m^2 + k_t^2} + 1 \right] &= \frac{\alpha_s(k_t^2)}{k_t^2} \ln \frac{Q^2 e^{-\frac{3}{2}}}{k_t^2} + \int_0^\infty \frac{dm^2 [\alpha_{\text{eff}}(m) - \alpha_s(k_t^2)]}{k_t^2 (m^2 + k_t^2)^2} \\ &= \frac{\alpha_s(k_t^2)}{k_t^2} \ln \frac{Q^2 e^{-\frac{3}{2}}}{k_t^2} + \mathcal{O}\left(\frac{\alpha_s^3(k_t^2)}{k_t^2}\right), \end{aligned} \quad (\text{A.23})$$

which completes the proof.

**Irrelevance of real-virtual mismatch.** One more comment is warranted concerning a mismatch between the phase space boundaries for the  $\alpha$ -integrations of the real and virtual contributions leading to (A.18). Namely, the virtual integral extends down to  $\alpha \geq \kappa_t^2$ , while the real one is cut off at  $\alpha \geq \kappa_t^2 + m^2$ . This tiny mismatch is nevertheless essential for the power correction analysis. Indeed, the difference of  $\alpha$ -integrals of the real and virtual contributions produces

$$\ln \frac{Q^2 e^{-\frac{3}{2}}}{\kappa_t^2 + m^2} - \ln \frac{Q^2 e^{-\frac{3}{2}}}{\kappa_t^2} = \ln \frac{\kappa_t^2}{\kappa_t^2 + m^2} = -\frac{m^2}{\kappa_t^2} + \dots \quad (\kappa_t^2 \gg m^2),$$

which gives rise to a logarithmically enhanced  $\mathcal{O}(m^2)$  contribution coming from the integration region  $m^2 \ll \kappa_t^2 \ll b^{-2}$ :

$$\int_0^{Q^2} \frac{d\kappa_t^2}{\kappa_t^2 + m^2} \ln \frac{\kappa_t^2(\kappa_t^2 + m^2)}{m^4} \ln \frac{\kappa_t^2}{\kappa_t^2 + m^2} [1 - J_0(b\kappa_t)] \simeq -\frac{b^2}{2} \cdot m^2 \int_{m^2}^{b^{-2}} \frac{d\kappa_t^2}{\kappa_t^2} \ln \frac{\kappa_t^2}{m^2}.$$

Taken at face value this would undermine the analysis of the quadratic power correction to the  $q\bar{q}$  EEC, since it seems to produce a logarithmically enhanced term of the order of  $m^2 \ln^2 m^2/Q^2$ . However, this non-cancellation occurs at the smallest kinematically allowed values of  $\alpha$ , which correspond to the values of the complementary Sudakov variable,  $\beta$ , at the edge of phase space where  $\beta = 1 - \mathcal{O}(m^2)$ . From the phase space (A.4) there is a suppression factor  $1 - \beta$  (coming from  $\zeta$ , see (A.5)) which degrades a contribution potentially non-analytic in  $m^2$  down to  $m^4$  at least. Therefore we can neglect this mismatch and not to worry about the fact that in this region neither (A.17) nor (A.15), which were based on soft gluon approximation, are valid.

## B. Quark-gluon contributions

By using the soft multi-parton distributions described in Appendix A, we derive here the quark-gluon distribution  $\mathcal{I}_{qg}(t)$  in the form given in (4.1). We recall that  $\mathcal{I}_{qg}(t)$  is obtained by integrating the partially inclusive quantity

$$H = \int d\omega_1(k_1) u(k_1) e^{i\vec{b}\vec{\kappa}_{t1}} + \int d\omega_2(k_1 k_2) [u(k_1) + u(k_2)] e^{i\vec{b}(\vec{\kappa}_{t1} + \vec{\kappa}_{t2})}, \quad (\text{B.1a})$$

$$u(k_i) = 2\alpha_i [\delta(t^2 - t_{k_i}^2) - \delta(t^2 - t_p^2)] ; \quad \text{with} \quad t_p = \frac{p}{Q}, \quad t_{k_i} = \frac{k_{ti}}{Q\alpha_i}. \quad (\text{B.1b})$$

In order to make explicit the finiteness of  $H$  and reconstruct the running coupling, we follow [11] and introduce an ‘‘inclusive source’’ (probing function)  $u'(k)$  to write

$$H = \int d\omega_1(k_1) u(k_1) e^{i\vec{b}\vec{\kappa}_{t1}} + \int d\omega_2(k_1 k_2) u'(k) e^{i\vec{b}\vec{\kappa}'_t} + \int d\omega_2(k_1 k_2) \left\{ [u(k_1) + u(k_2)] e^{i\vec{b}\vec{\kappa}_t} - u'(k) e^{i\vec{b}\vec{\kappa}'_t} \right\}, \quad (\text{B.2})$$

where in the last two terms  $k = k_1 + k_2$ , the momentum of the ‘‘parent gluon’’ with positive virtuality (mass)  $m$ . There is a freedom in the choice of the expression for the probing function  $u'(k)$  and transverse momentum  $\vec{\kappa}'_t$  describing the contribution to the EEC from a *massive* object. The only requirement is that in the  $m^2 \rightarrow 0$  limit  $u'(k) \exp(i\vec{b}\vec{\kappa}'_t)$  should coincide with the standard massless parton contribution  $u(k) \exp(i\vec{b}\vec{\kappa}_t)$  given in (B.1b). This ensures that for a collinear and infrared safe observable the difference vanishes for  $m^2 \rightarrow 0$ , thus making the last term in (B.2) finite

in the limit of collinear/soft parton splitting. The first two terms of (B.2) remain finite to all orders, as in the case of the radiator, due to the inclusive cancellation between the real and virtual corrections.

From [11] we know that the two-loop analysis can be greatly simplified if one defines  $u'(k)$  by replacing the *transverse momentum*,  $\kappa_t^2$ , in the definition of the massless source  $u(k)$  by the *transverse mass*,  $\kappa_t'^2 = \kappa_t^2 + m^2$ . Following this prescription we define

$$\begin{aligned} u'(k) &\equiv 2\alpha \left[ \delta(t^2 - t_k'^2) - \delta(t^2 - t_p^2) \right] , \\ \kappa_t'^2 &= \kappa_t^2 + m^2 , \quad k_t'^2 = (\vec{\kappa}_t' + \alpha\vec{p})^2 , \quad t_k' = \frac{k_t'}{\alpha Q} , \end{aligned} \quad (\text{B.3})$$

with  $\vec{\kappa}_t'$  and  $\vec{\kappa}_t$  parallel vectors. It is straightforward to verify that the difference of the probing functions in the last term of (B.2) vanishes for  $m^2 \rightarrow 0$ .

In Appendix C.2 we show that the PT component of  $\mathcal{I}_{qg}(t)$  gives a next-to-next-to-leading contribution. Here we discuss the NP component of  $\mathcal{I}_{qg}$  which provides the dominant power correction to EEC. We remark that it is legitimate to use the soft approximation, upon which (4.1) is based, to analyse the  $1/Q$  power contribution.

In [11] it was proposed to group the terms of (B.2) into three finite contributions,

$$\mathcal{I}_{qg}(t) = \mathcal{I}_0 + \mathcal{I}_{in} + \mathcal{I}_{ni} ,$$

the ‘‘naive’’, the ‘‘inclusive’’ and the ‘‘non-inclusive’’ contributions we shall now discuss.

**Naive contribution.** In the first term,  $\mathcal{I}_0$ , we reconstruct the running coupling as in the case of the radiator. This is done by combining the  $\alpha_s(0)$  term in  $\int d\omega_1(k) u(k)$  with the regular  $\beta_0$  part of the parent gluon source,  $\int d\omega_2(k_1 k_2) u'(k)$ , which emerges after integrating the gluon decay probability over the offspring variables, see (A.17). Similarly to the case of the radiator considered above, we reconstruct the effective coupling by using (3.2). The power contribution is then extracted by substituting the NP component of the effective coupling,  $\delta\alpha_{\text{eff}}$ , for  $\alpha_{\text{eff}}$ . One obtains

$$\mathcal{I}_0^{(\text{NP})}(t) = \frac{C_F}{\pi} \int_0^\infty dm^2 \delta\alpha_{\text{eff}}(m) \left( \frac{-d}{dm^2} \right) \int_0^\infty \frac{d^2\kappa_t}{\pi(\kappa_t^2 + m^2)} \Omega(\kappa_t^2 + m^2) . \quad (\text{B.4})$$

Due to our choice of  $k_t'$ , the trigger function  $\Omega_0$  is a function of the transverse mass,  $\kappa_t^2 + m^2$ , and is given by

$$\Omega(\kappa_t^2 + m^2) = \int \frac{d^2p}{2\pi} \int bdb e^{-\mathcal{R}(b)} J_0(bp) \int_0^1 2d\alpha \left[ \delta(t^2 - t_k'^2) - \delta(t^2 - t_p^2) \right] , \quad (\text{B.5})$$

where, in the leading (linear) approximation in  $m \sim \kappa_t \sim \alpha Q$ , we have omitted the  $b$ -dependence in the inclusive source (B.3). Invoking (3.10) we arrive at

$$\Omega(\kappa_t^2 + m^2) = 4 \int \frac{d^2t_p}{2\pi} \mathcal{I}(t_p) \int_0^1 d\alpha \left[ \delta(t^2 - t_k'^2) - \delta(t^2 - t_p^2) \right] , \quad (\text{B.6})$$

where we have invented the vector  $\vec{t}_p = \vec{p}/Q$ . Analogously one can introduce the vector  $\vec{t}'_k$  with modulus  $t'_k$  and arbitrary direction. Performing the integration over  $\kappa_t^2$  in (B.4) by parts, we obtain<sup>6</sup>

$$\mathcal{I}_0^{(\text{NP})}(t) = \frac{C_F}{\pi} \int_0^\infty dm^2 \delta\alpha_{\text{eff}}(m) \frac{\Omega(m^2)}{m^2}. \quad (\text{B.7})$$

As a result of the  $\kappa_t$  integration by parts we have  $\kappa_t = 0$ , and the relation (B.3),  $\vec{t}'_k = \vec{\kappa}'_t + \alpha\vec{p}$ , can be expressed as

$$\vec{t}'_k = \vec{t}_g + \vec{t}_p, \quad t_g = \frac{m}{\alpha Q}, \quad (\text{B.8})$$

the direction of  $\vec{t}_g$  being arbitrary.

To make explicit the  $m^2$  dependence of the trigger function  $\Omega(m^2)$  it is convenient to trade the  $\alpha$  integration for that over  $\vec{t}_g$  to arrive at

$$\Omega(m^2) = \frac{m}{Q} \rho(t), \quad \rho(t) = 2 \int \frac{d^2 t_g}{2\pi t_g^3} [\mathcal{I}_{q\bar{q}}(|\vec{t} - \vec{t}_g|) - \mathcal{I}_{q\bar{q}}(t)]. \quad (\text{B.9})$$

This equation has a clear physical meaning. The direction of the trigger is fixed to be  $\vec{t}$ . We have the standard logarithmic integration,  $d^2 t_g/t_g^2$ , with  $\vec{t}_g$  the direction of the gluer with respect to the radiating quark, weighted by the perturbative distribution over the quark direction,  $\vec{t}_p = \vec{t} - \vec{t}_g$ . The additional singular factor  $1/t_g$  comes from weighting by the gluer energy proportional to the ratio  $m/t_g$ , where  $m \sim \kappa_t \sim \Lambda$  is a typical finite transverse momentum scale determining the leading power contribution.

We conclude with the expression

$$\mathcal{I}_0^{(\text{NP})}(t) = \frac{2C_F}{\pi} \int dm \delta\alpha_{\text{eff}}(m) \cdot \rho(t) = \frac{2A_{1,0}}{Q} \cdot \rho(t). \quad (\text{B.10})$$

(For definition of the NP parameter  $A_{1,0}$  see Sect. 5.2.)

**Inclusive contribution.** The “inclusive” contribution  $\mathcal{I}_{in}(t)$  is obtained by summing the virtual correction  $\chi$  in  $\int d\omega_1(k) u(k)$ , see (A.14a), together with the logarithmically divergent part of  $\int d\omega_2(k_1 k_2) u'(k)$ , see (A.17). Its NP part is

$$\begin{aligned} \mathcal{I}_{in}^{(\text{NP})}(t) &= \frac{2C_A C_F}{\pi\beta_0} \int_0^\infty dm^2 \delta\alpha_{\text{eff}}(m) \left( \frac{-d}{dm^2} \right) \int_0^\infty \frac{d^2 \kappa_t}{\pi(\kappa_t^2 + m^2)} \ln \frac{\kappa_t^2(\kappa_t^2 + m^2)}{m^4} \Omega_{in}, \\ \Omega_{in} &\equiv \Omega(\kappa_t^2 + m^2) - \Omega(\kappa_t^2). \end{aligned} \quad (\text{B.11})$$

---

<sup>6</sup>Since only the terms non-analytic in  $m^2$  give non vanishing contributions to the  $m^2$  integral with  $\delta\alpha_{\text{eff}}$ , the actual ultraviolet limit of the  $\kappa_t$  integration,  $\kappa_t^2 < \kappa_{t\text{max}}^2 = \mathcal{O}(Q^2)$ , does not matter.



The effective coupling here has been introduced by using the relation between  $\alpha_{\text{eff}}$  and the dispersive density of the coupling  $\alpha_s$ , cf. (3.2),

$$\alpha_s(k) = - \int_0^\infty \frac{dm^2}{m^2 + k^2} \rho(m), \quad \rho(m) = \frac{d}{d \ln m^2} \alpha_{\text{eff}}(m) = -\beta_0 \frac{\alpha_s^2(m)}{4\pi} + \dots \quad (\text{B.12})$$

and by performing integration by parts.

**Non-inclusive contribution.** Applying to the combination  $\int d\omega_2(k_1 k_2) [u(k_1) + u(k_2) - u'(k)]$  in (B.2) the same procedure of replacing  $\alpha_s^2$  by the derivative of  $\alpha_{\text{eff}}$ , we present the NP part of the “non-inclusive” contribution,  $\mathcal{I}_{ni}$ , in the form

$$\begin{aligned} \mathcal{I}_{ni}^{(\text{NP})}(t) &= \frac{C_F}{\pi\beta_0} \int dm^2 \delta\alpha_{\text{eff}}(m) \left( \frac{-d}{dm^2} \right) \int \frac{d^2\kappa_t}{\pi} dz \frac{d\phi}{2\pi} M^2(k_1, k_2) \Omega_{ni}, \\ \Omega_{ni} &\equiv \Omega(\kappa_{t1}^2) + \Omega(\kappa_{t2}^2) - \Omega(\kappa_t^2 + m^2). \end{aligned} \quad (\text{B.13})$$

**Milan factor.** It is straightforward to verify that the combinations of trigger functions which enter into the inclusive and non-inclusive contributions are proportional, in the linear approximation, to the same function  $\rho(t)$  defined by (B.9), which determines the naive contribution:

$$\Omega_{in} = \Omega(\kappa_t^2 + m^2) - \Omega(m^2) \simeq \frac{\rho(t)}{Q} \cdot \left( \sqrt{\kappa_t^2 + m^2} - \kappa_t \right), \quad (\text{B.14})$$

$$\Omega_{ni} = \Omega(\kappa_{t1}^2) + \Omega(\kappa_{t2}^2) - \Omega(\kappa_t^2) \simeq \frac{\rho(t)}{Q} \cdot \left( \kappa_{t1} + \kappa_{t2} - \sqrt{\kappa_t^2 + m^2} \right). \quad (\text{B.15})$$

Such a structure is typical for the  $1/Q$  power corrections to various jet shapes and leads to the *universal* rescaling of the naive contribution (B.4) by the so-called Milan factor; for details see [20].

Taking account of the Milan factor, the full two-loop NP component of the  $qg$  contribution to the EEC becomes

$$\mathcal{I}_{qg}^{(\text{NP})}(t) = \mathcal{I}_0^{(\text{NP})}(t) \cdot \mathcal{M} = \frac{\lambda}{Q} \rho(t), \quad \lambda \equiv 2A_{1,0} \mathcal{M}. \quad (\text{B.16})$$

## C. Perturbative analysis of subleading corrections

### C.1 Single-log corrections to the radiator

In order to calculate  $\mathcal{R}^{(\text{PT})}$  with next-to-leading logarithmic accuracy we introduce the primitive function

$$\Phi(Q/\kappa_t) = \frac{2C_F}{\pi} \int_{\kappa_t}^Q \frac{dk}{k} \alpha_s^{\text{PT}}(k) \left( \ln \frac{Q^2}{k^2} - \frac{3}{2} \right), \quad (\text{C.1})$$

where  $\alpha_s^{\text{PT}}$  is defined here in the bremsstrahlung scheme. Writing  $\alpha_s = \alpha_s^{\text{PT}}(Q)$ ,  $\alpha = \alpha_s^{\text{PT}}(k)$  for brevity, we have to the required accuracy

$$\ln \frac{Q^2}{k^2} = \frac{4\pi}{\beta_0} \left( \frac{1}{\alpha_s} - \frac{1}{\alpha} + \frac{\beta_1}{4\pi\beta_0} \ln \frac{\alpha_s}{\alpha} \right), \quad (\text{C.2})$$

where

$$\beta_0 = 11 - 2n_f/3, \quad \beta_1 = 102 - 38n_f/3. \quad (\text{C.3})$$

Using the renormalization group equation, we can replace the  $k$ -integration by one with respect to  $\alpha$ :

$$\begin{aligned} \Phi(Q/k) &= \frac{16\pi C_F}{\beta_0} \int_{\alpha_s}^{\alpha} \frac{d\alpha}{\alpha(\beta_0 + \beta_1\alpha/4\pi)} \left( \frac{1}{\alpha_s} - \frac{1}{\alpha} + \frac{\beta_1}{4\pi\beta_0} \ln \frac{\alpha_s}{\alpha} - \frac{3\beta_0}{8\pi} \right) \\ &= \frac{16\pi C_F}{\beta_0^2} \left[ \frac{1}{\alpha} - \frac{1}{\alpha_s} + \frac{1}{\alpha_s} \ln \frac{\alpha}{\alpha_s} + \frac{\beta_1}{4\pi\beta_0} \left( \frac{\alpha}{\alpha_s} - 1 - \ln \frac{\alpha}{\alpha_s} + \frac{1}{2} \ln^2 \frac{\alpha}{\alpha_s} \right) - \frac{3\beta_0}{8\pi} \ln \frac{\alpha}{\alpha_s} \right]. \end{aligned}$$

Introducing

$$\ell_0 = \beta_0 \frac{\alpha_s}{2\pi} \ln \frac{Q}{k},$$

we have, to the required accuracy,

$$\frac{1}{\alpha} = \frac{1}{\alpha_s} (1 - \ell_0) + \frac{\beta_1}{4\pi\beta_0} \ln(1 - \ell_0). \quad (\text{C.4})$$

Integrating by parts we have

$$\begin{aligned} \mathcal{R}^{(\text{PT})}(b) &= \int_0^Q d\kappa_t [1 - J_0(b\kappa_t)] \frac{-d}{d\kappa_t} \Phi(Q/\kappa_t) \\ &= \int_0^{bQ} dx J_1(x) \Phi(bQ/x) + \mathcal{O}(\alpha_s(Q)), \quad x \equiv b\kappa_t, \end{aligned} \quad (\text{C.5})$$

where we have neglected the non-logarithmic correction  $\mathcal{O}(\alpha_s(Q))$  coming from the upper limit, which is taken care of by the coefficient function. Taking advantage of the fact that  $\Phi$  is a slowly varying function, we may substitute into (C.1) its logarithmic expansion,

$$\Phi(bQ/x) = \Phi(bQ) - \dot{\Phi}(bQ) \cdot \ln x + \mathcal{O}(\alpha_s(b^{-1})), \quad \dot{f}(z) = \frac{d}{d \ln z} f,$$

to obtain, with single-logarithmic accuracy,

$$\begin{aligned} \mathcal{R}^{(\text{PT})}(b) &= \Phi(bQ) - \dot{\Phi}(bQ) \int_0^\infty dx J_1(x) \ln x + \dots \\ &= \Phi(bQ) - \dot{\Phi}(bQ) (\ln 2 - \gamma_E) + \dots = \Phi\left(\frac{bQ}{2} e^{\gamma_E}\right) + \mathcal{O}(\alpha_s). \end{aligned} \quad (\text{C.6})$$

Putting everything together, we find

$$\begin{aligned} \mathcal{R}^{(\text{PT})}(b) = & -\frac{16\pi C_F}{\beta_0^2} \left[ \frac{1}{\alpha_s} (\ln(1-\ell) + \ell) + \frac{\beta_1}{4\pi\beta_0} \left( \frac{1}{2} \ln^2(1-\ell) + \frac{\ln(1-\ell) + \ell}{1-\ell} \right) \right. \\ & \left. - \frac{3\beta_0}{8\pi} \ln(1-\ell) - \frac{1}{2\pi} \left( \beta_0 \ln \frac{\mu}{Q} + K \right) \left( \ln(1-\ell) + \frac{\ell}{1-\ell} \right) \right] \end{aligned} \quad (\text{C.7})$$

where now

$$\ell = \beta_0 \frac{\alpha_s}{2\pi} \ln \frac{bQe^{\gamma_E}}{2}. \quad (\text{C.8})$$

Here we have allowed for an arbitrary renormalization scheme and renormalization scale  $\mu$ , so that now  $\alpha_s \equiv \alpha_s(\mu)$ , in both (C.7) and (C.8). The last term in Eq. (C.7) takes account of the scale and scheme dependence to two-loop accuracy. In the bremsstrahlung scheme  $K = 0$ , whereas in the  $\overline{\text{MS}}$  scheme one has

$$K = \frac{(67 - 3\pi^2)C_A - 10n_f}{18}. \quad (\text{C.9})$$

## C.2 Perturbative $qg$ contribution

To show that the  $qg$  correlation  $\mathcal{I}_{qg}(t)$  defined in (2.11) produces, at the PT level, a subleading  $\mathcal{O}(\alpha_s)$  correction to the EEC we consider the “naive” one-gluon contribution with the running coupling reconstructed as explained above. Measuring for brevity all momenta in units of  $Q$  we have

$$\begin{aligned} \mathcal{I}_{qg}^{(\text{PT})}(t) = & 2 \int \frac{d^2b d^2p}{(2\pi)^2} e^{i\vec{b}\vec{p}} e^{-\mathcal{R}(b)} \int \frac{d^2\kappa_t e^{i\vec{b}(\vec{\kappa}_t - \alpha\vec{p})}}{\pi(\vec{\kappa}_t - \alpha\vec{p})^2} \frac{C_F\alpha_s(\kappa_t)}{\pi} \\ & \times \alpha d\alpha P(\alpha) \vartheta(\alpha - \kappa_t) \left[ \delta\left(t^2 - \frac{\kappa_t^2}{\alpha^2}\right) - \delta(t^2 - p^2) \right] \\ = & \frac{C_F\alpha_s}{\pi} \int_0^\infty b db e^{-\mathcal{R}(b)} \int_0^1 \frac{d\kappa_t^2 dp^2}{|\kappa_t^2 - \alpha^2 p^2|} \int_0^1 \alpha d\alpha P(\alpha) \vartheta(\alpha - \kappa_t) \\ & \times J_0(bp(1-\alpha)) J_0(b\kappa_t) \left[ \delta\left(t^2 - \frac{\kappa_t^2}{\alpha^2}\right) - \delta(t^2 - p^2) \right]. \end{aligned} \quad (\text{C.10})$$

Since, as we shall see shortly, the  $\kappa_t$  integration is non-logarithmic, we have chosen to neglect the running and pulled out  $\alpha_s$  as a constant factor. Getting rid of the delta functions and defining the common “transverse momentum” integration variable  $q_t$  such that  $q_t = p$  for the first delta function, and  $q_t = \kappa_t/\alpha$  for the second one, we arrive at

$$\begin{aligned} \mathcal{I}_{qg}^{(\text{PT})}(t) \simeq & \frac{C_F\alpha_s}{\pi} \int_0^\infty b db e^{-\mathcal{R}(b)} \int_0^\infty \alpha d\alpha P(\alpha) \\ & \times \int_0^\infty \frac{dq_t^2}{|q_t^2 - t^2|} [J_0(bq_t(1-\alpha))J_0(bt\alpha) - J_0(bt(1-\alpha))J_0(bq_t\alpha)]. \end{aligned} \quad (\text{C.11})$$

Here we have substituted  $\infty$  for the actual upper limit of the  $q_t$  integration,  $q_t \lesssim 1$  (i.e.  $q_t \lesssim Q$ ), because the region  $q_t \gtrsim 1$  corresponds to small impact parameters  $b \leq 1$  ( $b \leq 1/Q$ ) and therefore produces a negligible contribution  $\mathcal{O}(t^2)$  to the answer for  $t \ll 1$ .

The  $\alpha$  and  $q_t$  integrals converge and produce no logarithmic enhancement. For the sake of simplicity we shall demonstrate this property by considering the  $qg$  contribution to the height of the ‘‘PT plateau’’, i.e. to the EEC distribution at  $t = 0$ . Setting  $t = 0$  we have

$$\begin{aligned} \mathcal{I}_{qg}^{(\text{PT})}(0) &= \frac{C_F \alpha_s}{\pi} \int_0^\infty b db e^{-\mathcal{R}(b)} \int_0^1 \alpha d\alpha P(\alpha) \int_0^\infty \frac{dq_t^2}{q_t^2} [J_0(bq_t(1-\alpha)) - J_0(bq_t\alpha)] \\ &= 2 \frac{C_F \alpha_s}{\pi} \int_0^\infty b db e^{-\mathcal{R}(b)} \int_0^1 d\alpha \left(-\frac{1}{2}\alpha\right) \cdot \ln \frac{\alpha}{1-\alpha} = -\frac{C_F \alpha_s}{2\pi} \int_0^\infty b db e^{-\mathcal{R}(b)}, \end{aligned} \quad (\text{C.12})$$

where we have used *antisymmetry* with respect to  $\alpha \leftrightarrow (1-\alpha)$  to substitute

$$2\alpha P(\alpha) = 1 + (1-\alpha)^2 = [2 - \alpha(1-\alpha)] - \alpha \implies (-\alpha),$$

and

$$\int_0^1 d\alpha \alpha \ln \frac{\alpha}{1-\alpha} = \frac{1}{2}.$$

We conclude that  $\mathcal{I}_{qg}^{(\text{PT})}$  amounts to a non-logarithmic  $\mathcal{O}(\alpha_s)$  correction to the quark-quark contribution (2.10):

$$\mathcal{I}_{qg}^{(\text{PT})}(0) \simeq \left[ -\frac{C_F \alpha_s}{\pi} \right] \cdot \frac{1}{2} \int_0^\infty b db e^{-\mathcal{R}(b)} = \left[ -\frac{C_F \alpha_s}{\pi} \right] \cdot \mathcal{I}_{q\bar{q}}^{(\text{PT})}(0). \quad (\text{C.13})$$

## D. Analytical estimates using one-loop coupling

We recall that the PT part of the radiator to single logarithmic accuracy is given by

$$\mathcal{R}^{(\text{PT})}(b) = \frac{4C_F}{\pi} \int_{1/\bar{b}}^Q \frac{d\kappa_t}{\kappa_t} \alpha_s(\kappa_t) \ln \frac{Qe^{-\frac{3}{4}}}{\kappa_t}, \quad \bar{b} = \frac{b e^{\gamma_E}}{2}, \quad (\text{D.1})$$

with  $\alpha_s$  the two-loop coupling in the bremsstrahlung scheme [14]. In this Appendix we study the EEC distribution neglecting  $\beta_1$ , the two-loop contribution to the running coupling. In so doing we lose control over single logarithmic contributions to the PT radiator, starting from  $\alpha_s^3 \log^3$ . On the other hand, this allows us to derive analytic expressions for the PT distribution and for the NP corrections to it. In particular we shall derive in this approximation the non-integer exponents of the  $Q$ -behaviour of the leading NP contributions to the EEC.

## D.1 Perturbative $q\bar{q}$ distribution

The PT radiator with the one-loop  $\alpha_s$  is

$$\mathcal{R}^{(\text{PT})}(b) = -c \left[ \left( L - \frac{3}{2} \right) \ln \frac{L - \ell}{L} + \ell \right], \quad (\text{D.2})$$

where

$$L \equiv 2 \ln \frac{Q}{\Lambda}, \quad \ell \equiv 2 \ln(Q\bar{b}),$$

and the numerical value of  $c$  is

$$c \equiv \frac{4C_F}{\beta_0} = \frac{16}{33 - 2n_f} = 0.5926, \quad \text{for } n_f = 3. \quad (\text{D.3})$$

The PT evaluation only makes sense for  $\ell < L$ , which implies

$$b < b_0 \equiv \frac{2e^{-\gamma_E}}{\Lambda}. \quad (\text{D.4})$$

The exponent of the radiator (D.2) has the following Mellin representation,

$$e^{-\mathcal{R}^{(\text{PT})}(b)} \vartheta(b_0 - b) = \int_{a-i\infty}^{a+i\infty} \frac{d\nu}{2\pi i} \left( \frac{b_0}{b} \right)^{2\nu} \cdot \frac{F(L)}{c + \nu} \left( \frac{c}{c + \nu} \right)^{c(L - \frac{3}{2})}, \quad a > 0, \quad (\text{D.5})$$

with

$$F(L) = e^{\frac{3}{2}c} \left( \frac{e}{cL} \right)^{c(L - \frac{3}{2})} \Gamma(1 + c(L - \frac{3}{2})) = \sqrt{2\pi cL} [1 + \mathcal{O}(L^{-1})].$$

The theta function on the left-hand side of (D.5) is ensured by the fact that the integrand has no singularities in the right half-plane, so that for  $b > b_0$  the  $\nu$ -contour can be moved to  $a \rightarrow \infty$ . Using

$$\int_0^\infty b db J_0(bt) \left( \frac{b_0}{b} \right)^{2\nu} = \frac{b_0^2}{2} \left( \frac{b_0 t}{2} \right)^{2(\nu-1)} \cdot \frac{\Gamma(1-\nu)}{\Gamma(\nu)}, \quad (\text{D.6})$$

we get

$$\mathcal{I}_{q\bar{q}}(t) = \frac{Q^2}{2} \int_0^{b_0} b db J_0(Qbt) e^{-\mathcal{R}^{(\text{PT})}(b)} = \int \frac{d\nu}{2\pi i} f(\nu, t), \quad (\text{D.7a})$$

$$f(\nu, t) = \frac{F(L)}{t^2(c + \nu)} \frac{\Gamma(1 - \nu)}{\Gamma(\nu)} \left( \frac{\Lambda^2 e^{\frac{3}{2}}}{Q^2} \right)^{c \ln \frac{c + \nu}{c}} \left( \frac{b_0 Q t}{2} \right)^{2\nu}. \quad (\text{D.7b})$$

Here we have extended the  $b$ -integral to infinity since the integrand represented by the right-hand side of (D.5) vanishes for  $b > b_0$ .

The inverse Mellin transform (D.7) can be formally evaluated by closing the  $\nu$ -contour around the poles of  $\Gamma(1 - \nu)$  at  $\nu = 1 + p$ , with  $p = 0, 1, \dots$ . For  $t = 0$  only

the pole at  $\nu = 1$  contributes and we derive the PT prediction for the height of the EEC distribution in the back-to-back region, see [5],

$$\mathcal{I}_{q\bar{q}}(0) = \frac{(b_0 Q)^2 F(L)}{4(c+1)} \left( \frac{\Lambda^2 e^{\frac{3}{2}}}{Q^2} \right)^{c \ln \frac{c+1}{c}} \simeq \frac{e^{-2\gamma_E}}{c+1} \sqrt{2\pi c \ln \frac{Q^2}{\Lambda^2}} \cdot \frac{Q^2}{\Lambda^2} \left( \frac{\Lambda^2 e^{\frac{3}{2}}}{Q^2} \right)^{c \ln \frac{c+1}{c}}. \quad (\text{D.8})$$

Making use of this result we can rewrite (D.7b) as

$$f(\nu, t) = \mathcal{I}_{q\bar{q}}(0) \frac{\Gamma(1-\nu)}{\Gamma(\nu)} \left( \frac{b_0 Q t}{2} \right)^{2(\nu-1)} \frac{c+1}{c+\nu} \left( \frac{\Lambda^2 e^{\frac{3}{2}}}{Q^2} \right)^{c \ln \frac{c+\nu}{c+1}} \quad (\text{D.9})$$

For  $t > 0$  all the poles ( $\nu = 1 + p$  with  $p = 0, 1, \dots$ ) contribute, and we obtain

$$\mathcal{I}_{q\bar{q}}(t) = \mathcal{I}_{q\bar{q}}(0) \sum_{p=0}^{\infty} \frac{(-1)^p}{(p!)^2} \left( \frac{b_0 Q t}{2} \right)^{2p} \frac{c+1}{c+1+p} \left( \frac{\Lambda^2 e^{\frac{3}{2}}}{Q^2} \right)^{c \ln \frac{c+1+p}{c+1}} \quad (\text{D.10})$$

This expansion is convergent for any  $(tQb_0)$ . However the series is oscillating, and for large  $(tQb_0)$  this representation is not suitable for practical computation.

## D.2 Full $q\bar{q}$ distribution

Taking account of the NP contribution to the radiator, the full quark-quark EEC is given by

$$\mathcal{I}_{q\bar{q}}(t) = \frac{Q^2}{2} \int b db J_0(Qbt) e^{-\mathcal{R}(\text{PT})(b)} e^{-\frac{1}{2}b^2\sigma} = \int_{a-i\infty}^{a+i\infty} \frac{d\nu}{2\pi i} f(\nu, t) \xi(\nu, t), \quad (\text{D.11})$$

with

$$\begin{aligned} \xi(\nu, t) &\equiv \int d^2t' \frac{e^{-t'^2/2\sigma}}{2\pi\sigma} \left( \frac{\vec{t} - \vec{t}'}{t} \right)^{2(\nu-1)} = \int_0^{2\pi} \frac{d\phi}{2\pi} \int_0^\infty \frac{dx^2}{x_0^2} e^{-x^2/x_0^2} (1+x^2+2x\cos\phi)^{\nu-1} \\ &= \sum_{n=0}^{\infty} \frac{x_0^{2n}}{n!} \left( \frac{\Gamma(\nu)}{\Gamma(\nu-n)} \right)^2; \quad x_0^2 \equiv \frac{2\sigma}{t^2}. \end{aligned} \quad (\text{D.12})$$

This function has no singularities in the finite  $\nu$ -plane. Taking the contributions from the poles in  $f(\nu, t)$  we obtain the two equivalent expansions

$$\begin{aligned} \mathcal{I}_{q\bar{q}}(t) &= \mathcal{I}_{q\bar{q}}(0) \cdot \sum_{p=0}^{\infty} \frac{(-1)^p}{(p!)^2} \left( \frac{b_0 Q t}{2} \right)^{2p} \frac{c+1}{c+1+p} \left( \frac{\Lambda^2 e^{\frac{3}{2}}}{Q^2} \right)^{c \ln \frac{c+1+p}{c+1}} X_p(t), \\ &= \mathcal{I}_{q\bar{q}}(0) \cdot \sum_{p=0}^{\infty} \frac{(-1)^p}{(p!)^2} \left( \frac{b_0 Q t}{2} \right)^{2p} \frac{c+1}{c+1+p} \left( \frac{\Lambda^2 e^{\frac{3}{2}}}{Q^2} \right)^{c \ln \frac{c+1+p}{c+1}} Y_p, \end{aligned} \quad (\text{D.13})$$

where

$$X_p(t) = \sum_{n=0}^p \frac{1}{n!} \left( \frac{2\sigma}{(tQ)^2} \right)^n \left( \frac{p!}{(p-n)!} \right)^2 = 1 + p^2 \frac{2\sigma}{(tQ)^2} + \dots \quad (\text{D.14})$$

and

$$\begin{aligned} Y_p &= \sum_{n=0}^{\infty} \frac{(-\frac{1}{2}b_0^2\sigma)^n}{n!} \frac{c+1+p}{c+1+p+n} \left( \frac{\Lambda^2 e^{\frac{3}{2}}}{Q^2} \right)^{c \ln \frac{c+1+p+n}{c+1+p}} \\ &= 1 - \frac{1}{2}b_0^2\sigma \frac{c+1+p}{c+2+p} \left( \frac{\Lambda^2 e^{\frac{3}{2}}}{Q^2} \right)^{c \ln \frac{c+2+p}{c+1+p}} + \dots \end{aligned} \quad (\text{D.15})$$

In particular,  $Y_0$  gives the height of the plateau at  $t = 0$  for the full distribution, relative to the PT prediction (D.8):

$$\mathcal{I}_{q\bar{q}}(0) = \mathcal{I}_{q\bar{q}}(0) \cdot \sum_{n=0}^{\infty} \frac{(-\frac{1}{2}b_0^2\sigma)^n}{n!} \frac{c+1}{c+1+n} \left( \frac{\Lambda^2 e^{\frac{3}{2}}}{Q^2} \right)^{c \ln \frac{c+1+n}{c+1}}. \quad (\text{D.16})$$

The exponents of successive power terms slowly increase; their magnitudes oscillate and decrease factorially. For  $n_f = 3$  we have numerically

$$\begin{aligned} \frac{\mathcal{I}_{q\bar{q}}(0)}{\mathcal{I}_{q\bar{q}}(0)} &= 1 - 0.307 (b_0^2\sigma) \left( \frac{\Lambda^2 e^{\frac{3}{2}}}{Q^2} \right)^{0.289} + 0.0554 (b_0^2\sigma)^2 \left( \frac{\Lambda^2 e^{\frac{3}{2}}}{Q^2} \right)^{0.482} + \dots \\ &= 1 - 0.597 \frac{\sigma}{\Lambda^2} \left( \frac{\Lambda}{Q} \right)^{0.578} + 0.182 \left( \frac{\sigma}{\Lambda^2} \right)^2 \left( \frac{\Lambda}{Q} \right)^{0.964} + \dots \end{aligned} \quad (\text{D.17})$$

### D.3 NP $qg$ contribution

The NP part of  $\mathcal{I}_{qg}(t)$  is given by the convolution

$$\delta\mathcal{I}_{qg}(t) = \frac{2\lambda}{Q} \int \frac{d^2x}{2\pi x^3} [\mathcal{I}_{q\bar{q}}(\vec{t} - \vec{x}) - \mathcal{I}_{q\bar{q}}(t)] = \frac{2\lambda}{tQ} \int \frac{d\nu}{2\pi i} f(\nu, t) \zeta(\nu), \quad (\text{D.18})$$

with

$$\begin{aligned} \zeta(\nu) &= \int_0^\infty \frac{dx}{x^2} \int_0^{2\pi} \frac{d\psi}{2\pi} [(1 + x^2 + 2x \cos \psi)^{\nu-1} - 1] \\ &= \int_0^1 dx \int_0^{2\pi} \frac{d\phi}{2\pi} \left\{ \frac{(1 + x^2 + 2x \cos \psi)^{\nu-1} - 1}{x^2} + \frac{(1 + x^2 + 2x \cos \psi)^{\nu-1}}{x^{2(\nu-1)}} - 1 \right\}. \end{aligned} \quad (\text{D.19})$$

The latter representation leads to the series expansion

$$\zeta(\nu) = \sum_{k=0}^{\infty} \left( \frac{\Gamma(\nu)}{\Gamma(\nu-k)k!} \right)^2 \left( \frac{1}{2k-1} - \frac{1}{2(\nu-k)-3} \right). \quad (\text{D.20})$$

Observing that under the exchange  $k \rightarrow \nu - k - 1$  the first factor is symmetric and the second is antisymmetric, we conclude that  $\zeta(\nu)$  vanishes at the positive integer points  $\nu = 1 + p$ ,  $p = 0, 1, \dots$ , thus cancelling the poles of the PT function  $f(\nu, t)$ .

The only remaining singularities of the  $\nu$ -integrand in (D.18) are the poles of  $\zeta(\nu)$  at  $\nu = \frac{3}{2} + p$  with  $p = 0, 1, \dots$ . Evaluating the Mellin transform by closing the contour around these poles we get an expansion similar to that for the PT distribution  $\mathcal{I}_{q\bar{q}}(t)$ ,

$$\delta\mathcal{I}_{qg}(t) = -2\lambda b_0 \cdot \mathcal{I}_{q\bar{q}}(0) \cdot \sum_{p=0}^{\infty} \frac{(-1)^p}{(p!)^2} \left(\frac{b_0 Q t}{2}\right)^{2p} \frac{c+1}{c+\frac{3}{2}+p} \left(\frac{\Lambda^2 e^{\frac{3}{2}}}{Q^2}\right)^{c \ln \frac{c+\frac{3}{2}+p}{c+1}}. \quad (\text{D.21})$$

In particular, we immediately obtain for the leading NP correction to the plateau height ( $n_f = 3$ )

$$\frac{\delta\mathcal{I}_{qg}(0)}{2\lambda b_0 \mathcal{I}_{q\bar{q}}(0)} = -\frac{c+1}{c+\frac{3}{2}} \left(\frac{\Lambda^2 e^{\frac{3}{2}}}{Q^2}\right)^{c \ln \frac{c+\frac{3}{2}}{c+1}} = -0.970 \left(\frac{\Lambda^2}{Q^2}\right)^{0.1618}. \quad (\text{D.22})$$

#### D.4 Full EEC

Putting together the quark-quark and the quark-gluon contributions to the EEC we have

$$\begin{aligned} \mathcal{I}_{tot}(t) &\equiv \mathcal{I}_{q\bar{q}}(t) + \mathcal{I}_{qg}(t) = \int \frac{d\nu}{2\pi i} f(\nu, t) \left\{ \zeta(\nu) + \frac{2\lambda}{tQ} \xi(\nu, t) \right\} \\ &= \mathcal{I}_{q\bar{q}}(0) \cdot \sum_{p=0}^{\infty} \frac{(-1)^p}{(p!)^2} \left(\frac{b_0 Q t}{2}\right)^{2p} \frac{c+1}{c+1+p} \left(\frac{\Lambda^2 e^{\frac{3}{2}}}{Q^2}\right)^{c \ln \frac{c+1+p}{c+1}} Z_p, \end{aligned} \quad (\text{D.23})$$

where

$$Z_p \equiv 1 - 2\lambda b_0 \frac{c+1+p}{c+\frac{3}{2}+p} \left(\frac{\Lambda^2 e^{\frac{3}{2}}}{Q^2}\right)^{c \ln \frac{c+\frac{3}{2}+p}{c+1+p}} - \frac{1}{2} b_0^2 \sigma \frac{c+1+p}{c+2+p} \left(\frac{\Lambda^2 e^{\frac{3}{2}}}{Q^2}\right)^{c \ln \frac{c+2+p}{c+1+p}} + \dots \quad (\text{D.24})$$

Setting  $t = 0$  we derive the leading NP power suppressed contributions to the height of the plateau ( $n_f = 3$ )

$$\begin{aligned} \frac{\mathcal{I}_{tot}(0)}{\mathcal{I}_{q\bar{q}}(0)} &= 1 - 1.57 b_0 \lambda \left(\frac{\Lambda e^{\frac{3}{4}}}{Q}\right)^{0.323} - 0.307 (b_0^2 \sigma) \left(\frac{\Lambda e^{\frac{3}{4}}}{Q}\right)^{1.16} + \dots \\ &= 1 - 2.25 \frac{\lambda}{\Lambda} \left(\frac{\Lambda}{Q}\right)^{0.323} - 0.922 \frac{\sigma}{\Lambda^2} \left(\frac{\Lambda}{Q}\right)^{1.16} + \dots \end{aligned} \quad (\text{D.25})$$

where  $\mathcal{I}_{q\bar{q}}(0)$  is the perturbative plateau in (D.8). The first NP correction comes from the quark-gluon and the second from the quark-quark correlation.



## References

- [1] C.L. Basham, L.S. Brown, S.D. Ellis and S.T. Love, *Phys. Rev. Lett.* **41** (1978) 1585; *Phys. Rev. D* **19** (1979) 2018.
- [2] G. Sterman and S. Weinberg, *Phys. Rev. Lett.* **39** (1977) 1436.
- [3] Yu.L. Dokshitzer, D.I. Dyakonov and S.I. Troyan, *Phys. Lett.* **B 84** (1979) 234, *Phys. Rep.* **C 58** (1980) 270;  
G.Parisi and R.Petronzio, *Nucl. Phys.* **B 154** (1979) 427;  
J. Kodaira and L. Trentadue, *Phys. Lett.* **B 123** (1983) 335.
- [4] J.C. Collins and D.E. Soper, *Nucl. Phys.* **B 193** (1981) 381, Erratum *ibid.* **B 213** (1983) 545; *ibid.* **B 197** (1982) 446; *Phys. Rev. Lett.* **48** (1982) 655.
- [5] P. Rakow and B.R. Webber, *Nucl. Phys.* **B 187** (1981) 254.
- [6] J.C. Collins and D.E. Soper, *Acta Phys. Polon.* **B 16** (1985) 1047; *Nucl. Phys.* **B 284** (1987) 253.
- [7] A.V. Manohar and M.B. Wise, *Phys. Lett.* **B 344** (1995) 407 [hep-ph/9406392];  
G.P. Korchemsky and G. Sterman, *Nucl. Phys.* **B 437** (1995) 415 [hep-ph/9411211];  
B.R. Webber, *Phys. Lett.* **B 339** (1994) 148; see also *Proc. Summer School on Hadronic Aspects of Collider Physics*, Zuoz, Switzerland, August 1994, ed. M.P. Locher (PSI, Villigen, 1994) [hep-ph/9411384];  
M. Beneke and V.M. Braun, *Nucl. Phys.* **B 454** (1995) 253 [hep-ph/9506452];  
Yu.L. Dokshitzer and B.R. Webber, *Phys. Lett.* **B 352** (1995) 451 [hep-ph/9504219];  
R. Akhoury and V.I. Zakharov, *Phys. Lett.* **B 357** (1995) 646 [hep-ph/9504248]; *Nucl. Phys.* **B 465** (1996) 295 [hep-ph/9507253];  
Yu.L. Dokshitzer, V.A. Khoze and S.I. Troyan, *Phys. Rev. D* **53** (1996) 89 [hep-ph/9506425]; P. Nason and B.R. Webber, *Phys. Lett.* **B 395** (1997) 355 [hep-ph/9612353];  
G.P. Korchemsky, G. Oderda and G. Sterman, in *Deep Inelastic Scattering and QCD*, 5<sup>th</sup> International Workshop, Chicago, IL, April 1997, p. 988 [hep-ph/9708346].
- [8] Yu.L. Dokshitzer, Plenary talk at 29th ICHEP–98, Vancouver, Canada, July 1998 [hep-9812252].
- [9] Yu.L. Dokshitzer, G. Marchesini and B.R. Webber, *Nucl. Phys.* **B 469** (1996) 93 [hep-ph/9512336].
- [10] Yu.L. Dokshitzer, V.A. Khoze, A.H. Mueller and S.I. Troyan, *Basics of Perturbative QCD*, ed. J. Tran Thanh Van, Editions Frontières, Gif-sur-Yvette, 1991.
- [11] Yu.L. Dokshitzer, A. Lucenti, G. Marchesini and G.P. Salam, *Nucl. Phys.* **B 511** (1998) 396 [hep-ph/9707532].
- [12] V.N. Gribov and L.N. Lipatov, *Sov. Phys. JETP* **15** (1972) 438, 675.

- [13] J. Kodaira and L. Trentadue, *Phys. Lett.* **B 112** (1982) 66.
- [14] S. Catani, G. Marchesini and B.R. Webber, *Nucl. Phys.* **B 349** (1991) 635.
- [15] G. Turnock, Cambridge preprint Cavendish-HEP-92/3; Cambridge University Ph.D. thesis, 1992.
- [16] UA5 Collaboration, G.J. Alner et al., *Nucl. Phys.* **B 291** (1987) 445.
- [17] B.R. Webber, in *Proc. Hadronic aspects of collider physics, Zuoz 1994*, p. 49, [hep-ph/9411384].
- [18] S. Catani and M.H. Seymour *Nucl. Phys.* **B 485** (1997) 291, Erratum *ibid.* **B 510** (1997) 503; program obtainable from <http://hepwww.rl.ac.uk/theory/seymour/nlo/>.
- [19] M. Dasgupta, G.E. Smye and B.R. Webber *J. High Energy Phys.* **04** (1998) 017 [hep-ph/9803382].
- [20] Yu.L. Dokshitzer, A. Lucenti, G. Marchesini and G.P. Salam, *J. High Energy Phys.* **05** (1998) 003 [hep-ph/9802381].
- [21] M. Dasgupta and B.R. Webber, *Eur. Phys. J.* **C 1** (1998) 539 [hep-ph/9704297]; *J. High Energy Phys.* **10** (1998) 001 [hep-ph/9809247].
- [22] O. Biebel, *Nucl. Phys. Proc. Suppl.* **64** (1998) 22 [hep-ex/9708036];  
D. Wicke, *ibid.* **64** (1998) 27 [hep-ph/9708467];  
J. C. Thompson, ALEPH collab., contribution to Europhysics HEP Conference, Jerusalem, Israel, August 1997 [hep-ex/9812004];  
C. Adloff et al., H1 collab., *Phys. Lett.* **B 406** (1997) 256 [hep-ex/9706002];  
29<sup>th</sup> ICHEP–98, Vancouver, Canada, July 1998, contribution # 530;  
P.A. Movilla Fernandez et al., JADE collab., *Eur. Phys. J.* **C 1** (1998) 461 [hep-ex/9708034];  
talk at QCD Euroconference, Montpellier, France, July 1998, [hep-ex/9808005];  
talk at 29<sup>th</sup> ICHEP–98, Vancouver, Canada, July 1998 [hep-ex/9807007].
- [23] M. Dasgupta and B.R. Webber, *Phys. Lett.* **B 382** (1996) 273 [hep-ph/9604388].
- [24] B.R. Webber, *J. High Energy Phys.* **10** (1998) 012 [hep-ph/9805484].
- [25] PLUTO Collaboration: C. Berger et al., *Phys. Lett.* **B 99** (1980) 292.
- [26] SLD Collaboration: K. Abe et al. *Phys. Rev.* **D 51** (1995) 962.
- [27] OPAL Collaboration: P.D. Acton et al., *Zeit. Phys.* **C 59** (1993) 1.
- [28] P. Ball, M. Beneke and V.M. Braun, *Nucl. Phys.* **B 452** (1995) 563 [hep-ph/9502300].
- [29] F.E. Low, *Phys. Rev.* **D 110** (1958) 974 ;  
T.H. Burnett and N.M. Kroll, *Phys. Rev. Lett.* **20** (1968) 86.